2016-09-13

Proteomics of Human Dendritic Cell Subsets Reveals Subset-Specific Surface Markers and Differential Inflammasome Function.

Worah, K

10.1016/j.celrep.2016.08.023
Cell Rep
Elsevier BV

This is an accepted manuscript of an article pubblished by Elsevier in Cell Reports (accepted August 5 2016) available at:

http://dx.doi.org/10.1016/j.celrep.2016.08.023

==========

Proteomics of Human Dendritic Cell Subsets Reveals Subset-Specific Surface Markers and Differential Inflammasome Function

Kuntal Worah[1,#], Till S. Mathan[1,#], Thien Phong Vu Manh[6], Shivakumar Keerthikumar[3,7], Gerty Schreibelt[1], Jurjen Tel[1] , Tjitske Duiveman-de Boer[1], Annette E. Sköld[1,8], Annemiek B. van Spriel[1], I. Jolanda M de Vries[1,2], Martijn A. Huynen[3], Hans J. Wessels[4,5], Jolein Gloerich[4] , Marc Dalod[6] , Edwin Lasonder[3,9$], Carl G. Figdor[1$], Sonja I. Buschow[1,10].

[1]Departments of [1]Tumor Immunology, and , [2]Medical Oncology, Radboud Institute for Molecular Life Sciences**,** [3]Centre for Molecular and Biomolecular Informatics (CMBI) [4]Radboud Proteomics Centre, Department of Laboratory Medicine, [5]Nijmegen Centre for Mitochondrial Disorders, Radboud University Medical Center, PO Box 9101, 6500 HB Nijmegen, The Netherlands

[6]Centre d'Immunologie, de Marseille-Luminy, Aix Marseille University UM2, Inserm, U1104, CNRS UMR7280, F-13288 Marseille Cedex 09, France

[7]Present Address: Department of Biochemistry and Genetics, La Trobe Institute for Molecular Science, La Trobe University, Melbourne, Victoria, 3086, Australia

[8]Department of Oncology-Pathology, Karolinska University Hospital Solna, Karolinska Institutet, Stockholm, Sweden

[9]School of Biomedical and Healthcare Sciences, B427 Portland Square, Plymouth University, Drake Circus, Plymouth, Devon PL4 8AA, United Kingdom.

[10]Department of Gastroenterology and Hepatology, Erasmus MC-University Medical Center, Rotterdam,3015 CN, Rotterdam, The Netherlands

[$] Authors contributed equally

[#]Co-first author

Correspondence: S.Buschow@erasmusmc.nl, Carl.Figdor@radboudumc.nl

Abbreviations:

Dendritic cell (DC), plasmacytoid DC (pDC), myeloid DC (mDC), Toll like receptors (TLR), C-type lectin receptors (CLR), Pattern recognition receptors (PRR), Mass spectrometry (MS), Liquid Chromatography-MS/MS (LC-MS/MS), Label free quantification (LFQ), Differentially expressed protein (DEP), Differentially expressed gene (DEG).

SUMMARY

Dendritic cells (DCs) play a key role in orchestrating adaptive immune responses. In human blood, three distinct subsets exist: plasmacytoid DCs (pDCs) and BDCA3+ and CD1c+ myeloid DCs. In addition, a DClike CD16+ monocyte has been reported. Although RNA-expression profiles have been previously compared, protein expression data may provide a different picture. Here, we exploited label-free quantitative mass spectrometry to compare and identify differences in primary human DC subset proteins. Moreover, we integrated these proteomic data with existing mRNA data to derive robust cell-specific expression signatures with more than 400 differentially expressed proteins between subsets, forming a solid basis for investigation of subset-specific functions. We illustrated this by extracting subset identification markers and by demonstrating that pDCs lack caspase-1 and only express low levels of other inflammasome related proteins. In accordance, pDCs were incapable of interleukin (IL)-1b secretion in response to ATP.

INTRODUCTION

Dendritic cells (DCs) play a critical role in the initiation of antigen specific adaptive immune responses to foreign antigens and the maintenance of tolerance to self-antigens (reviewed by Balan et al., 2014; Reynolds and Haniffa, 2015; Vu Manh et al., 2015). DCs harbor the unique capacity to process and present antigens complexed to either major histocompatibility complex (MHC) class I or MHC class II and thereby can activate naive T cells. It is because of this ability that DCs have become of interest as tools or targets for cancer immunotherapy to initiate or boost tumor immunity.

Several DC subsets can be distinguished that differ in their ability to sense and respond to pathogens and in the type of immune response they initiate. Two main types of naturally occurring blood DCs have been characterized: plasmacytoid DCs (pDCs) and myeloid DCs (mDCs) (reviewed by Vu Manh et al.,2015). pDCs play a key role in antiviral immunity, through their ability to produce large amounts of type I interferons (IFNs). mDCs represent the ‘‘traditional’’ antigen-presenting DCs that can be further subdivided based on the expression of BDCA3 (CD141) and CD1c (BDCA1). Each can be defined through the expression of different pattern recognition receptors (PRRs; e.g., Toll-like receptors [TLRs] and C-type lectin receptors [CLRs]) and the secretion of a distinct set of cytokines upon stimulation (reviewed by Balan et al., 2014; Reynolds and Haniffa, 2015; Vu Manh et al., 2015). Whereas CD1c+ mDCs express most TLRs, except TLR9, BDCA3+ mDCs express mainly TLR3. Furthermore, BDCA3+ mDCs express the CLR CLEC9a, which facilitates the uptake of dying cells and subsequent cross-presentation of derived antigens to T cells (Ahrens et al., 2012; Jongbloed et al., 2010; Poulin et al., 2010). Finally, although not considered a genuine DC, a CD16+ subset of monocytes, coined ‘‘non-classical monocytes,’’ can be found in blood with DC-like properties (Ziegler-Heitbrock et al., 2010). So far, these DCs subsets have been mostly characterized and isolated based on cell-specific (surface) markers and functionally compared for abilities such as antigen presentation, cytokine secretion, and migration (Balan et al., 2014; Reynolds and Haniffa, 2015; Vu Manh et al., 2015). These functional assays, however, can be biased as they provide information on only a few a priori determined functional responses to a limited set of activation stimuli and antigens. Although highly valuable in investigating the abilities of each

subset under specific circumstances, these assays may leave more untraditional unique characteristics of each subset undetected. To overcome this, unbiased analyses of mRNA expression of human and mouse DC subsets have been performed and proven to be highly informative (Lindstedt et al., 2005; Manh et al., 2013; Miller et al., 2012; Robbins et al., 2008). Comparative transcriptome analysis delivered the most compelling evidence for the current thought that the human BDCA3+ mDC is the counterpart of the murine CD8a+ DC, despite the lack of conservation of identification markers (Robbins et al., 2008). In addition, the Robbins et al. (2008) study demonstrated that the CD16+ DC-like cell, based on its full transcriptional program, resembles a monocyte more than a DC. Although these studies have provided valuable insight into the relation between DC subsets in mice and humans, RNA expression does not always reflect protein expression. Since not all RNA is translated, RNA and proteins may have dissimilar half-lives and kinetics, and protein levels may also be regulated by post-transcriptional modifications. Furthermore transcriptomics does not take into account pre-existing protein levels, alterations in translation efficiency, or protein stability. Therefore, transcriptome expression data may have limited predictive power on which proteins really define each DC subset and may have left important phenotypic and functional differences unnoticed. To confirm and supplement the existing transcriptome analysis, we have performed a comprehensive mass-spectrometry (MS)-based quantitative proteome comparison of rare blood DC subsets. Furthermore, we integrated protein and RNA data to derive expression signatures that give a more reliable and comprehensive account of expression differences than can be achieved from using either technique alone. The expression signatures represent an easily accessible resource to derive hypotheses on subset-specific functions. To illustrate this, we validated five of the identified differentially expressed surface markers and showed that caspase-1 is completely lacking in pDCs, which is accompanied by restricted expression of other inflammasome components and affects the function of these cells.

RESULTS

Quantitative Proteomics of Primary Human DC Subsets

For proteome characterization, four DC-(like) subsets (i.e., pDCs, CD1c+ mDCs, BDCA3+ mDCs, and CD16+ monocytes) were isolated from apheresis products obtained from healthy volunteers by magnetic-bead-based cell separation. The purity of the isolated cells and presence of cross-contamination were assessed by flow cytometry (Figure S1). For pDCs, CD1c+ mDCs, and CD16+ monocytes, high purity (R95%) was obtained for all subsets without major cross-contamination or presence of B or T cells in two out of three donors. For a third donor, medium-high purity was obtained (78%–92%). For BDCA3+ mDC samples, most cells were BDCA3+CD11c+ (87%–95%). We observed however, a variable number of CD11c+ cells expressing intermediate levels of BDCA3 (BDCA3int) in the isolate together with cells positive for CD1c+, indicating cross-contamination of this sample with CD11c+CD1c+BDCA3int cells. Therefore, we consider these samples to be BDCA3+ mDC enriched rather than pure. Nevertheless, we reasoned that this sample is still of use to derive BDCA3+ mDC-specific protein expression, which may be achieved by relating the BDCA3+ mDC-enriched samples to the (BDCA3+-depleted) CD1c+ mDC samples. All 12 (three donors times four subsets) samples were, first, each separated using SDS-PAGE, fractionated into 20 fractions, and subjected to in-gel trypsin digestion (yielding 240 fractions in total). The fractions were measured in triplicate, using highly sensitive liquid chromatography-tandem MS (LC-MS/MS) for maximal protein coverage. After peptide identification and sequence alignment, proteins were quantified using the label free quantification (LFQ) algorithm in MaxQuant (Cox et al.,2014). The Pearson correlation was very high ($r = 0.97 \pm 0.02$) between technical replicates and high ($r = 0.93 \pm 0.02$) between biological replicates (e.g., the same subsets from different donors), indicating good reproducibility across measurements and donors (Table S1). In total, we identified 42,723 non-redundant peptide sequences corresponding to 4,196 protein groups (Table S2; Table S3). Requiring a protein to be expressed in at least two donors for each subset, we identified 2,351, 2,197, 2,009, and 1,883 proteins in pDCs, BDCA3+ mDCs, CD1c+ mDCs, and CD16+ cells, respectively, and 2,823 proteins overall (Figures S2A–S2D; Tables S2 and S3). Next, using the CORUM database of protein complexes, we inspected the identification of components of protein complexes essential for cell

homeostasis (e.g., mitochondrial complexes and proteasomes), to assess the completeness of the proteome in each cell type (Luber et al., 2010). We recovered most components, indicating that our proteome covered the majority of DC proteins (Figure S2E). Coverage was best in pDCs and BDCA3+ mDCs, yielding 70%–100% of essential protein complexes, and was least in CD16+ cells (40%–100%; Figure S2E).

We then evaluated the assignment of key identification markers for each subset. No markers specific for other major leukocyte populations (e.g., T, B, or NK cells) were identified, suggesting a lack of substantial contamination with other leukocytes. In contrast, we readily identified the unique expression of at least one previously reported subset-specific protein for each subset, including TLR7, TLR9, CLEC4C, NRP1, and IL3RA for pDCs; IDO and HLA-DO for BDCA3+ mDCs; and CD16 (FCGR3A) for CD16+ monocytes (Table 1). Importantly, CD1c was uniquely detected in CD1c+ mDCs but not in BDCA3+ mDCs. For BDCA3+ DCs, we did not immediately identify more traditional markers such as BDCA3 (CD141, THBD), CLEC9a, TLR3, NECL2, and XCR1 using the default peptide identification threshold (false discovery rate [FDR] = 0.01). Possibly, this was due to a low expression, high hydrophobicity, or heavy glycosylation of these molecules. Nevertheless, we found a unique expression of IDO and HLA-DO in BDCA3+ mDCs; they were previously reported to be highly expressed in especially this subset (Crozat et al., 2010; Hornell et al., 2006). Upon more close inspection of peptides, however, TLR3 was found in one BDCA3+ mDC sample, and CLEC9A and BDCA3 (CD141 / THBD) were found in two samples. Because these peptides were detected with low confidence (FDR = 1), we generated MS/MS spectra and manually verified this result (data not shown). Together, the expression patterns of established marker proteins demonstrate the ability of our approach to discern the distinct identity of each subset.

We also obtained quantitative information using the LFQ algorithm in MaxQuant (Cox et al., 2014). First, we used this information to compare protein expression in the three main populations of blood DC-like cells (i.e., pDCs, CD1c+ mDCs, and CD16+ monocytes), excluding the BDCA3+ mDC samples. We calculated average expression differences between any two subsets and visualized these in volcano plots (Figure 1A; see Table S4 for complete statistical analysis). It should be noted that here and in the remainder of the manuscript, only proteins expressed in at least

two donors in one of the cell types being compared are included. Pairwise comparisons further highlighted subset identity, showing specific expression of CD11c (ITGAX/ITGB2) in myeloid cells and overexpression in the pDCs of several proteins with a reported pDC-specific expression and function (e.g., PACSIN1, SLC14A4, IRF7, TCF4, BCL11A, BLNK, and CD2AP) (Blasius et al., 2010; Cisse et al., 2008; Crozat et al., 2010; Esashi et al., 2012; Marafioti et al., 2008; Robbins et al., 2008; Rock et al., 2007; Wu et al., 2013).

Next, we determined the relation between cell types by hierarchical clustering (Figure 1B). Based on all proteins, subsets clustered together mostly on cell type rather than on donor. Furthermore, CD16+ monocytes and CD1c+ mDCs that share a myeloid origin were closer to each other than to pDCs. Hierarchical clustering of samples based on 1,218 differentially expressed proteins (DEPs) between the three subsets showed a separation similar to that seen when using all proteins and indicated six main groups of DEPs that showed higher or lower expression in one of the three subsets (Figure 1C). Next, we assessed how our protein data related to mRNA data. We merged our protein data with a previously published and publicly available microarray dataset of the same subsets (Lindstedt et al., 2005). For one of the donors that was used for MS analysis, we also acquired sufficient material to perform RNA sequencing on the same sample (Table S5). We first assessed the overall correlation between microarray-derived RNA data and proteome data for each cell type and found this to be low, similar to our previous observations (Figure 1D; r = 0.28–0.31) (Buschow et al., 2010). The correlation between RNA-sequencing data and proteome data for the matched donor was slightly better (0.37–0.45). Cross-correlation of this RNA-sequencing dataset to the protein data of the two other donors, however, produced a similar correlation, indicating that the different RNA analysis method was mostly responsible for the improved correlation (Table S6). To make a more in-depth comparison of the RNA data to our proteome dataset possible, we transformed both microarray-derived RNA and protein expression data to relative expression levels for each dataset separately (Z scores, mean to 0, variance to 1). From the merged dataset, we yielded 742 DEPs for which also RNA data were available. Again, we used the merged RNA and protein data for these 742 DEPs as input for hierarchical clustering (Figure 1E; Table S6). The combined protein and RNA samples grouped the distinct subsets from the two datasets together, indicating

that, despite moderate correlation between absolute expression levels, there was a good correlation between RNA and protein expression patterns (Figure 1E). Importantly, the clustering was determined neither by biological variation between donors nor by technical variation between omics technologies.

Generation of Protein-Based Expression Signatures and Networks

Protein and RNA data were not consistent in all cases, and proteome analysis put forward DEPs for which differences at the RNA level were only minor or for which no probes had been present on the microarray chips. Next, we set out to visualize were exactly proteome analysis pointed to not previously appreciated differences between DC subsets and the cases in which RNA and protein were in agreement. For the six groups of DEPs associated with the three subsets (Figure 1C), we generated protein expression signatures based on four different evidence levels: (I) subset-specific protein expression/absence, supported by RNA data; (II) differential protein expression between subsets, supported by RNA data; (III) subset-specific protein expression/ absence, not supported by RNA data; and (IV) differential protein expression between subset, not supported by RNA data (Figure 2; Supplemental Experimental Procedures). Proteins included in signatures based on level I and level II evidence behaved consistently in RNA and protein datasets. These proteins are, thus, likely mostly regulated at the transcriptional level. Importantly, for these proteins, proteomics data confirmed RNA-identified differences between subsets. Many established markers were present in these two groups: e.g., IL3RA, CLEC4C, TLR9, CD1c, and FCGR3B (CD16). Supported by two lines of evidence, other proteins in these groups now represent high-potential subset identification markers and include CD163 for CD1c+ mDCs and SIGLEC10 for CD16+ monocytes (Figure 2; Table S7). In contrast, proteins included in signatures based on level III and level IV evidence reflect less consistency between protein and RNA expression patterns or a lack of transcriptional information/ChIP (chromatin immunoprecipitation) annotation. Proteins in these evidence groups represent the added value of the proteome analysis (Figure 2). Finally, proteins that were put forward as differentially expressed by RNA data (differentially expressed genes; DEGs), and that were also

present in our protein dataset but were not confirmed as differentially expressed by proteomics, are listed in Table S8.

Together, we confirmed differential or unique expression of 253 proteins between the three subsets previously observed by RNA expression (pDCs, 109 higher/65 lower; CD1c+ mDCs, 17 higher/1 lower; CD16+ monocytes, 34 higher/27 lower) that could also be derived from the transcriptome data (levels I and II; Figure 3; Table S7, including lower confidence DEPs). In addition, 143 proteins were found to be differently/uniquely expressed between subsets based on proteomics data only (levels III and IV), which hold yet-unappreciated differences between DC subsets (pDCs, 75 higher/14 lower; CD1c+ mDCs, 10 higher/8 lower; CD16+ monocytes, 10 higher/26 lower). To obtain insight into the overall function of signature proteins, we performed a protein-protein interaction (PPI) analysis and a functional annotation (FA) analysis (Figure 3; Table S9). PPI analysis demonstrated good connectivity between proteins high in pDCs (0.73 connection per protein), proteins low in pDCs (1 connection per protein), those high in CD1c+ mDCs (0.85 connection per protein), and those low in CD16+ monocytes (0.64 connection per protein) (Figure 3; Table S9). Much less connectivity was found between proteins high in CD16+ monocytes (0.25 connection per protein) and those low in CD1c+ mDCs (no connections were identified).

In the CD1c+ mDC high signature, the MCM family and accessory proteins that regulate the cell cycle were found by proteome analysis only and were highly connected, suggesting a unique role for this complex in CD1c+ mDCs (Figure 3; Table S9). This complex was completely absent from CD16+ monocytes. Proteome analysis, but not RNA analysis, also pointed out that CD1c+ mDCs more highly expressed both the alpha-chain and the beta-chain of HLA-DQ, which may, thus, be of specific importance in this DC subset. The largest gene signatures were obtained for pDCs and mostly mapped to expected pDC functions, including TLR and IFN signaling (e.g., TLR9, IRF7, IRF8, and SMAD3), but also to endoplasmic reticulum (ER), Golgi, and vesicular transport, indicating high protein biosynthesis in this cell type (e.g., SEC24A, SEC31A, SEC11C, PDIA5, PDIA4, ERGIC3, and LMAN1) (Figure 3; Table S9). Intriguingly, IFN and TLR signalling pathway constituents were highly expressed in pDCs by both RNA and protein analyses, while proteins involved in protein biosynthesis and vesicular transport were, in many cases, highly

expressed at the protein level only (Figure 3). The proteins absent from pDCs (e.g., shared by CD1c+ mDCs and CD16+ monocytes) were also highly connected and related to cell adhesion and protrusion formation (e.g., ZYX, MSN, PAK1, VASP, and FSCN1; Table S9), in line with the rounder non-adhesive phenotype of pDCs. Furthermore, pDCs hardly expressed or even lacked TLR2, which detects bacterial lipoproteins, several proteins connected to bactericidal endo/phagosomes (e.g.,HMOX1, NCF2, and RAB27a) and CASP1 (caspase-1), a crucial enzyme in the inflammasome-induced cleavage of interleukin (IL)-1b in macrophages and DCs (Figure 3; Table S9).

BDCA3+ versus CD1c+ mDCs

Next, we investigated the difference between the two myeloid DC subsets. Despite the presence of CD1c+ mDCs in the BDCA3+ mDC samples, mDC samples were largely devoid of other blood cells (Figure S1). Importantly, CD1c+ mDC samples were devoid of BDCA3+ mDCs. A direct comparison between the two sets of samples could, therefore, still reveal important expression differences between mDC subsets (Figure 4; Table S4). As expected, the number of DEPs between BDCA3+ mDCs and CD1c+ mDCs was much less than between other subsets, reflecting the presence of CD1c+ cells in both samples and/or their more common origin. Similar to what we found before, protein only moderately correlated to RNA expression ($r = 0.31$ for microarray or $r = 0.38$ for RNA sequencing; Figure 4B; Table S6). Despite the contamination with CD1c+ mDCs, the BDCA3+ mDC protein samples clustered with the microarray RNA samples of BDCA3+ mDCs, indicating that the cross-contamination did not mask BDCA3+ mDC subset identity (Figure 4C). Finally, we derived DEPs between BDCA3+ mDCs and CD1c+ mDCs, using integration of protein and RNA data (Figures 4D and 4E). DEPs included IDO1, FUCA1, CD93, HLA-DOB, and TAP2 (high in BDCA3 mDCs) and also SIRPA, SIGLEC9, and CASP1 (high in CD1c+ mDCs). Several more DEGs by microarray showed a similar trend at the protein level but did not meet our stringent criteria (e.g., IRF8, CAMK2D, and TAP1; Table S8). Others were not found differentially expressed by proteomics or even showed an opposite trend.

Validation of DEPs

To demonstrate the resource value of our integrated proteome and RNA analysis, we selected five cell-surface receptors for validation. We chose cell-surface receptors because these may reflect the ability of each subset to recognize dangerous agents, and could aid subset identification by flow cytometry. Using the latter technique, we confirmed differential expression of all five receptors: SIRPa and Siglec-9 were found on CD16+ monocytes and CD1c+ mDCs only; CD93 was especially high on BDCA3+ mDCs; Siglec-10 was unique to CD16+ monocytes; and, finally, CD163 was high on CD1c+ mDCs (Figure 5).

Absence of Caspase-1 in pDCs Reflects Low Inflammasome Activity

Previous transcriptome analysis already indicated that pDCs express lower levels of transcripts for proteins involved in antibacterial innate immune responses (Crozat et al., 2009). It was not clear whether this also translated to protein expression and functionality. Our proteome data now confirm that pDCs express lower levels of or lack TLR2, NAIP, HMOX, RAB27A, NCF2, and CASP1 (Figure 2; Table S7). Caspase-1, a crucial player in inflammasome function, was abundantly present in CD1c+mDCs and CD16+ cells but was lacking in pDCs (Figure 6A). In the BDCA3+ mDC-enriched sample, caspase-1 was present but at much lower levels than in CD1c+ mDCs. Importantly, protein quantification was based on 6, 11, or even 13 peptides for BDCA3+ mDCS, CD1c+ mDCs, or CD16+ monocytes, respectively, while in pDCs, only a single peptide was mapped to caspase-1 that was not adequate for quantification, suggesting the absence or very low expression of this protein (Table S3). To further substantiate these MS data, we analyzed protein expression by western blot (WB). Caspase-1 was readily detected in CD1c+ mDCs and CD16+ monocytes but was present only at very low levels in pure BDCA3+ mDCs and not at all detected in pDCs (Figures 6B and S4). It should be noted that we did detect low levels of caspase-1 in pDCs isolated by magnetic beads but that protein expression was completely absent when cells were sorted to high purity (>99%) by flow cytometry (Figures 6 and S4). We next wondered whether pDCs would upregulate caspase-1 when activated. To test this, we incubated cells with the TLR7/8 ligand R848. Cell activation by TLR stimulation upregulated caspase-1 in CD1c+ mDCs but did not in pDCs (Figures 6C and S4). CD16+ monocytes also did

not further increase caspase-1 expression upon TLR stimulation. Upregulation of caspase-1 in BDCA3+ DCs could not be tested, because we did not manage to isolate a sufficient number of cells to test both resting and stimulated conditions by WB.

Next, we were interested in the expression of other components of the inflammasome pathway. Only very few other proteins of this pathway were identified by MS: NAIP was also detected in all subsets except for pDCs, while the inflammasome- component NLRC4 was identified in CD16+ monocytes only (Figure 2; Table S7). Exploration of the publicly available RNA expression data, however, indicated that low expression in pDCs was not restricted to caspase-1 but also included most other inflammasome components, as stated previously (Crozat et al., 2009). CD16+ monocytes, in contrast, expressed high levels of inflammasome constituents, CD1c+ mDCs expressed more moderate levels, and BDCA3+ mDCs expressed low levels (Figure 6D). Together, these data strongly suggest an overall low presence of inflammasome-related proteins in pDCs. Consequently, pDCs may not be equipped to recognize inflammasome-activating stimuli or to synthesize and secrete IL-1b in response. All components of the pathway downstream of ATP recognition were low in pDCs compared to the other subsets (P2XR7, PANX, NLRP3, CARD8, PYCARD, and CASP1; Figure 6D), indicating that pDCs may not be equipped to respond to this danger-associated molecule. ATP can trigger the cleavage and secretion of IL-1b, provided that necrosis factor kB (NFkB) signaling is present at the same time to induce pro-IL-1b expression. As a proof of principle, we tested the ability of subsets to secrete IL-1b in response to ATP, preceded by 4-hr or overnight R848 stimulation to trigger NF-kB signaling via TLR7/8. Upregulation of activation marker CD83 and/or production of tumor necrosis factor a (TNF-a) was observed in all DC subsets, demonstrating functional NF-kB signaling (Figures 6E–6G). IL-1b secretion was restricted to especially CD1c+mDCs and CD16+ mDCs. Thus, these data confirm that pDCs, indeed, lack IL-1b secretion in response to ATP. Of note, IL-18, which also requires caspase-1 for secretion, was readily secreted by ATP/R848-stimulated CD1c+ mDCs but not by pDCs (Figure S4). BDCA3+ mDCs were clearly activated by R848, as judged by the increased expression of CD83, yet hardly produced any cytokines (including IL-1b) under these circumstances (Figures 6E–6G).

These experiments together demonstrate that the inflammasome/ caspase-1 pathway is present and functional in CD1c+ mDCs and CD16+ monocytes but not in pDCs. Concordantly, pDCs do not secrete IL1b in response to ATP.

DISCUSSION

This study describes an elaborate proteome analysis of human blood-derived DC subsets and provides DC subset-specific protein signatures. This dataset holds unique information on the differences between DC subsets and reveals which differences, previously identified using mRNA, are really present at the protein level. Previously, Luber and colleagues analyzed the proteome of murine DC subsets (Luber et al., 2010), but large-scale proteomics of human DCs was thus far restricted to in-vitro generated monocyte-derived DCs (moDCs) and CD1c+ mDCs (Buschow et al., 2010; Schlatzer et al., 2012). The latter study reported 725 proteins expressed in resting and TLR-stimulated CD1c+ mDCs together, of which the majority (75%) was also identified, in the present analysis, in resting CD1c+ mDCs, along with a further 1,500 other proteins. The present dataset thus represents, to the best of our knowledge, the most complete quantitative proteome analysis of human DC subsets and provides a unique side-by-side comparison of these cells from the same donors.

We report on nearly 400 differentially expressed proteins between the three main blood DC-like subsets. In addition, despite the presence of CD1c+ mDCs in the BDCA3+ mDC sample, we identify over 60 proteins differentially expressed between mDC subsets, of which we subsequently validated four by flow cytometry. The protein-based signatures we derived provide insight into possible functional differences between subsets. Although we cannot discuss in detail all the functional implications of the expression differences we have identified, several warrant further discussion. First, we demonstrate the abundant expression of the MCM family of proteins in CD1c+mDCs, but not in CD16+ monocytes or in pDCs. This protein family is essential for cell division. Thus, our data support previous findings that, in contrast to pDCs, a fraction of the blood mDC population may still be able to expand, possibly reflecting an incomplete differentiation state (Segura et al., 2012). Our data suggest that, like pDCs, CD16+ cells may completely lack the potential to expand. The remaining capacity of mDCs to divide is interesting from a clinical perspective, as it implies that mDCs after isolation may have the potential to be further expanded.

This concept may be of interest for the development of immunotherapies for cancer or chronic inflammatory diseases, where obtaining sufficient cell numbers is still a major hurdle.

Second, HLA (human leukocyte antigen) molecule expression demonstrated some marked differences between subsets, suggesting subset-specific antigen presentation. CD1c+ mDCs not only highly express antigen-presenting CD1c but also highly expressed HLA-DQ, as compared to pDCs and CD16+ monocytes (but not HLA-DR). In agreement with a previous report, BDCA3+ cells uniquely expressed HLA-DO (Hornell et al., 2006). For these HLA types, either a clear (HLA-DO) or a unique (HLA-DQ versus HLA-DR) biological function remains to be defined. Thus, the consequence of this subset-specific expression remains elusive. Third, many ER- and Golgi-located proteins were expressed at higher levels, specifically in pDCs. Previously, it has been shown that, in mice, pDCs and, to a lesser extent, CD8a+ DCs (the supposed murine equivalent of BDCA3+ DCs), were reported to display a constitutive activation of the unfolded protein response (UPR), as was indicated by the alternative splicing of XBP1 (Iwakoshi et al., 2007). The increase in UPR was required for ER expansion to facilitate rapid IFN-a biosynthesis and is reminiscent of plasma cell differentiation (Iwakoshi et al., 2007). The high levels of ER and glycoprotein biosynthesis and transport proteins that we describe in pDCs support the paradigm that immature pDCs are already prepared for rapid IFN-a synthesis. Proteins related to intracellular protein transport machinery are also overtly expressed in immature pDCs, and these may provide important clues to unravel the largely unknown IFN-a secretory route.

From the identified DEPs, we confirmed five cell-surface receptors by flow cytometry: SIRPa and Siglec-9, which bind to CD47 and sialic acids, respectively, were found to be highly expressed on both CD16+ monocytes and CD1c+ mDCs. These receptors share a capacity to limit DC function and inflammation and are exploited by bacteria and malignant cells to evade immune responses (Laubli et al., 2014; Ohta et al., 2010; Barclay and Van den Berg, 2014). Lack of these receptors may render cells insensitive to this evasion. CD1c+ mDCs uniquely expressed CD163, a scavenger receptor and PRR for bacteria (Kristiansen et al., 2001; Fabriek et al., 2009). Siglec-10, which we found selectively expressed on CD16+ monocytes, is a putative adhesion receptor and PRR that has been reported to be expressed on CD16+ but

not CD16 monocytes, as well as on moDCs (Ancuta et al., 2009; Kivi et al., 2009; Li et al., 2001; Stephenson et al., 2014). Finally, BDCA3+ mDCs highly expressed CD93, which was reported to mediate phagocytosis and clearance of apoptotic cells and, as such, may act as an accessory to CLEC9A (Nepomuceno and Tenner, 1998; Norsworthy et al., 2004).

Our proteome data provided strong evidence for a lack of caspase-1 in pDCs. We validated this by WB and show data to suggest that pDCs have a diminished presence of inflammasome pathway constituents. Concordantly, pDCs did not respond to inflammasome activator ATP, while CD1c+ mDCs and CD16+ monocytes did. Our data contradict those of several previous studies reporting on IL1-b secretion by pDCs (Hurst et al., 2009; Yu et al., 2010). These studies show pDCs to secrete pictograms of IL1b per milliliter of culture supernatant in response to TLR stimulation alone (without inflammasome activation). However, this level of IL1b is extremely low compared to production by CD16+ monocytes, which, we found, can secrete over a 100- fold more (nanograms of) IL1b per milliliter upon TLR and inflammasome stimulation. Furthermore, it is conceivable that traces (e.g., ±1%) of high IL1b-producing cells may be present in these pDC preparations isolated by magnetic beads, and such cells can contribute to the low amount of IL1b found to be secreted.

Interestingly, our proteome data also indicated that, although expression of caspase-1 was readily detected in the BDCA3+- enriched samples by proteomics, it was lower than in CD1+ mDCs and CD16+ DCs, a result we also verified using highly pure cells. Indeed, BDCA3+ mDCs responded less to inflammasome activation in the presence of TLR7/8 ligand. This stimulus matured BDCA3+ mDCs but did not induce cytokine secretion. However, low IL1-b production by BDCA3+ mDCs relative to CD1c+ mDCs, in response to the potent BDCA3+ mDC-activating stimulus poly(I:C), has also been reported (Jongbloed et al., 2010).

Several recent publications have demonstrated that the pDC hallmarks type I IFN and IRF7 may directly inhibit IL-1b and inflammasome activity (Guarda et al., 2011; Salem et al., 2011). In pDCs, TLR7 activation by hepatitis C virus induced type I IFN secretion but induced neither IL-1b nor IL-18. In contrast, TLR7 activation in monocytes induced IL-1b and IL-18, rather than type I IFN (Chattergoon et al., 2014;

Dreux et al., 2012). The differentiation program involving IRF7 that allows pDCs to secrete large amounts of type I IFN may, thus, downregulate inflammasome pathway constituents, including caspase-1. Although this causal relation still awaits further experimental confirmation, this could switch the pDC response to TLR stimulation/NF-kB activation away from IL-1b and toward type I IFNs. A switch between type I IFNs and IL-1b could serve to prevent excessive damaging inflammation during antiviral responses.

Taken together, the proteome dataset that we describe provides a rich resource to solidly establish the phenotypic and functional capacities of human DC subsets and to decipher the contribution of each subset to the initiation of immune responses.

EXPERIMENTAL PROCEDURES

Cells

DCs were isolated from apheresis products obtained from healthy volunteers after written informed consent was obtained and according to institutional guidelines and overseen by the local institutional review board (Commissie mensgebonden onderzoek [CMO]). Peripheral blood mononuclear cells (PBMCs) were purified via Ficoll density gradient centrifugation (Lucron Bioproducts), followed by magnetic-bead (Miltenyi Biotec) or flow-cytometric isolation, and were directly lysed for MS or WB analysis or were used in in vitro experiments (see the following text and Supplemental Experimental Procedures for details).

LC-MS/MS

In brief: Tryptic peptides were analyzed using LC (Easy-nLC; Thermo Fisher Scientific) coupled to a 7-T linear ion trap Fourier-transform ion cyclotron resonance mass spectrometer model (LTQ FT Ultra, Thermo Fisher Scientific). See Supplemental Experimental Procedures for details.

MS Data Processing

Proteins were identified and quantified from raw mass spectrometric files using MaxQuant software, version 1.3.0.5 (Cox and Mann, 2008). A database search was performed in the Andromeda search engine (Cox et al., 2011) against the Human Uniprot database (86,749 entries, June 2012). The protein abundance was determined by MaxLFQ, as described by Cox et al. (2014). The MS proteomics data have been deposited to the ProteomeXchange Consortium via the PRIDE partner repository with the identifier PRIDE: PXD004678 (Vizcaıno et al., 2016). (http://proteomecentral.proteomexchange.org). See Supplemental Experimental Procedures for details.

Statistical Analysis of Protein and RNA Data

See the Supplemental Experimental Procedures for details. Statistical analysis was performed in the R programming environment. Data were visualized using GENE-E software (http://www.broadinstitute.org/cancer/software/ GENE-E) and BioLayout Express3D (version 3.3) (Theocharidis et al., 2009). For PPI analysis, we used the STRING PPI web tool (version 10; http:// string-db.org/), and FA analysis was done using the DAVID web tool (https:// david.ncifcrf.gov/).

Western Blotting and ELISA

These were performed according to standard procedures. See Supplemental Experimental Procedures for details and antibodies used.

In Vitro DC Activation

Isolated DC-like subsets were resuspended in X-VIVO 15 (Cambrex) containing 2% pooled human serum (Sanquin). pDCs were supplemented with 10 ng/ml recombinant human IL-3 (rhIL-3; Cellgenix). Both cell types were stimulated for 4 hr or overnight with 4 mg/ml R848, followed by 45-min stimulation with 5 mM ATP (Sigma). Culture supernatant was taken for ELISA.

ACCESSION NUMBERS

The accession number for the MS proteomics data reported in this paper is PRIDE: PXD004678.

SUPPLEMENTAL INFORMATION

Supplemental Information includes Supplemental Experimental Procedures, four figures, and nine tables and can be found with this article online at http://dx.doi.org/10.1016/j.celrep.2016.08.023.

AUTHOR CONTRIBUTIONS

Conceptualization, S.I.B.; Methodology, S.I.B., E.L., and M.D.; Investigation, K.W., T.S.M., G.S., J.T., T.D.-d.B., and A.E.S.; Formal Analysis, K.W., T.P.V.M., and S.K.; Writing – Original Draft, K.W. and S.I.B.; Writing – Review & Editing, M.D., E.L., A.B.v.S., and C.G.F; Visualization, K.W. and T.S.M.; Funding Acquisition, C.G.F.; Resources, I.J.M.d.V., J.G., and H.J.W.; Supervision, S.I.B., E.L., C.G.F, M.D., and M.A.H.

ACKNOWLEDGMENTS

The authors thank John-Paul Jukes for critical reading of the manuscript. This work was supported by a grant from the Dutch Cancer Society (KUN2009- 4402), a Radboudumc RIMLS PhD grant, and grants from the Netherlands Organisation for Scientific Research (951.03.002 and 822.02.017). J.T. received grant NWO-Veni 863.13.024. A.B.v.S. received grant NWO-Vidi 864.11.006. I.J.M.d.V. received grant NWO-Vici 918.14.655. C.G.F. received the NWO Spinoza grant and ERC Adv grant PATHFINDER (269019).

Legends

Table 1. Subset identification markers uniquely identified.

The numbers of peptide identified and quantified for each marker protein for each subsets. Shown markers were not identified in any of the other subsets for all donors. aPeptides were detected by releasing the FDR threshold of 0.01 and for which peptide spectra were manually validated.

Figure 1. Comparison of protein expression between 3 main blood DC-like subsets and integration with RNA data.

(A) Volcano plots depicting protein expression differences (x-axis: 2log fold change) and the significance level (y-axis: -10log (t-test p-value)) comparing the indicated 3 subsets. Coloured dots represent proteins with a fold change of >2 and $p<0.05$ while gray dots represent proteins that did not match these criteria. Proteins specific to one of the 2 subsets compared were assigned a fold change of infinity. (See also Table S4) (B) Unsupervised hierarchical clustering of DC subsets using all proteins identified in at least 2 donors of at least one subset. (1-Pearson correlation) (C) Clustering of subsets based on 1218 DEPsby 3-group one-way ANOVA ($p<0.05$) or specifically expressed in one subtype in at least two donors. (D) Pearson correlation for each subtype between protein and RNA (microarray) expression levels (E)Hierarchical clustering of merged transcriptome and proteome data (DEPs only). (See also Table S5 and Figure S5.)

Figure 2. Cell specific gene signatures derived from proteomics and transcriptomics.

Protein based gene signatures for higher or lower expression in the three main subsets were derived from the merged proteome and transcriptome data based on 4 levels of evidence: I) Specific protein expression/ absence for withRNA support II), differential protein expression with RNA support III), specific protein expression without RNA support and lastly IV) differential protein expression without RNA support. Proteins marked by asterisks were specifically identified by MS in two donors only but were included because of RNA support (e.g. “rescued”). The heat

map colors represent the relative protein expressionin each DC subsetand donor. (See also Table S5.)

Figure 3. Signature protein-protein interaction networks highlight functional differences between subsets.

Signatures were used as input for STRING analysis (confidence level 0.4) to visualize possible connections between proteins. (See also Table S9.) Proteins indicated in blue were included based on protein and RNA data and red protein were pointed out by protein data only(see also methods and table S5). Important biological functions of sections of each network are indicated (based on functional enrichment see Table S9).

Figure 4. Pairwise comparison of BDCA3+ mDCs and CD1c+ mDCs.

(A) Volcano plot depicting protein expression differences (x-axis: 2log fold change) and the significance level (y-axis: -10log (t-test p-value) as in figure 1. (B) Pearson correlation between protein and RNA (microarray)expression levels for all proteins. (C) Hierarchical clustering of merged z-scored transcriptome and proteome data of DEPs. (See also Table S6). (D) Heat map of the relative protein expression (LFQ) of proteins identified to be specifically (Level I and III) or differentially expressed (Level II or IV; by t-test), based on protein and RNA data evidence (Level I and II) or protein evidence only (Level III and IV).

Figure 5. Confirmation of differentially expressed surface markers.

(A) Representative histogram of the expression of indicated surface markers by specific antibodies (lines) or isotype controls (grey area) on the 4 DC-like subsets. (B) Bar diagrams summarizing the specific fluorescence level measured by flow cytometry (FC) in 4 novel healthy donors (isotype control antibody signal subtracted). Mean ± SEM of 4 healthy donors. All markers were found differentially expressed by one-way ANOVA ($p<0.05$), and with indicated significance by post-hoc Tukey's Multiple Comparison Test *$p<0.05$, **$p<0.01$, *** <0.001. (C) Bar diagrams of mean LFQ values as obtained by MS analysis (3 donors).

Figure 6. Absence of Caspase and inflammasome activity in pDCs.

(A) Bar diagrams of LFQ values for Caspase-1 as obtained by MS analysis (3 donors). (B &C) Western blot analysis of DC subsets isolated by flow sorting from two novel donors lysed directly after isolation or (C) also afterovernight stimulation with R848. Shown is the signal for Caspase-1 and actin that were probed sequentially on the same blotting membrane. (D) Heat map of 2log intensity values of probes mapping to inflammasome components derived from microarray data of the 4 subsets from 3 donors. (E) Flow cytometry based evaluation of the surface expression of the maturation marker CD83 on immature or ATP stimulated (4 hours 45 min) subsets. Results of a representative donor are shown. (D & E) Secretion of indicated cytokines by pDCs and CD1c mDC after stimulation for 4 hours (D) or overnight (E) with R848 followed by 45 min with ATP by ELISA. Results are the mean values ± SEM obtained with cells from at least 4 donors. Significance of the effect of stimulation on each subset and cytokine was evaluated by a two-tailed Mann-Whitney test. *p<0.05, **p<0.01, *** <0.001, ns=non-significant.

REFERENCES

Ahrens, S., Zelenay, S., Sancho, D., Hanc, P., Kjaer, S., Feest, C., Fletcher, G., Durkin, C., Postigo, A., Skehel, M.*, et al.* (2012). F-actin is an evolutionarily conserved damage-associated molecular pattern recognized by DNGR-1, a receptor for dead cells. Immunity *36*, 635-645.

Ancuta, P., Liu, K.Y., Misra, V., Wacleche, V.S., Gosselin, A., Zhou, X., and Gabuzda, D. (2009). Transcriptional profiling reveals developmental relationship and distinct biological functions of CD16+ and CD16- monocyte subsets. BMC Genomics *10*, 403.

Balan, S., Ollion, V., Colletti, N., Chelbi, R., Montanana-Sanchis, F., Liu, H., Vu Manh, T.P., Sanchez, C., Savoret, J., Perrot, I.*, et al.* (2014). Human XCR1+ dendritic cells derived in vitro from CD34+ progenitors closely resemble blood dendritic cells, including their adjuvant responsiveness, contrary to monocyte-derived dendritic cells. Journal of immunology *193*, 1622-1635.

Blasius, A.L., Arnold, C.N., Georgel, P., Rutschmann, S., Xia, Y., Lin, P., Ross, C., Li, X., Smart, N.G., and Beutler, B. (2010). Slc15a4, AP-3, and Hermansky-Pudlak syndrome proteins are required for Toll-like receptor signaling in plasmacytoid dendritic cells. Proceedings of the National Academy of Sciences of the United States of America *107*, 19973-19978.

Buschow, S.I., Lasonder, E., van Deutekom, H.W., Oud, M.M., Beltrame, L., Huynen, M.A., de Vries, I.J., Figdor, C.G., and Cavalieri, D. (2010). Dominant processes during human dendritic cell maturation revealed by integration of proteome and transcriptome at the pathway level. Journal of proteome research *9*, 1727-1737.

Chattergoon, M.A., Latanich, R., Quinn, J., Winter, M.E., Buckheit, R.W., 3rd, Blankson, J.N., Pardoll, D., and Cox, A.L. (2014). HIV and HCV activate the inflammasome in monocytes and macrophages via endosomal Toll-like receptors without induction of type 1 interferon. PLoS pathogens *10*, e1004082.

Cisse, B., Caton, M.L., Lehner, M., Maeda, T., Scheu, S., Locksley, R., Holmberg, D., Zweier, C., den Hollander, N.S., Kant, S.G.*, et al.* (2008). Transcription factor E2-2 is an essential and specific regulator of plasmacytoid dendritic cell development. Cell *135*, 37-48.

Cox, J., Hein, M.Y., Luber, C.A., Paron, I., Nagaraj, N., and Mann, M. (2014). Accurate proteome-wide label-free quantification by delayed normalization and maximal peptide ratio extraction, termed MaxLFQ. Mol Cell Proteomics *13*, 2513-2526.

Cox, J., and Mann, M. (2008). MaxQuant enables high peptide identification rates, individualized p.p.b.-range mass accuracies and proteome-wide protein quantification. Nat Biotechnol *26*, 1367-1372.

Cox, J., Neuhauser, N., Michalski, A., Scheltema, R.A., Olsen, J.V., and Mann, M. (2011). Andromeda: a peptide search engine integrated into the MaxQuant environment. Journal of proteome research *10*, 1794-1805.

Crozat, K., Guiton, R., Guilliams, M., Henri, S., Baranek, T., Schwartz-Cornil, I., Malissen, B., and Dalod, M. (2010). Comparative genomics as a tool to reveal functional equivalences between human and mouse dendritic cell subsets. Immunological reviews *234*, 177-198.

Crozat, K., Vivier, E., and Dalod, M. (2009). Crosstalk between components of the innate immune system: promoting anti-microbial defenses and avoiding immunopathologies. Immunological reviews *227*, 129-149.

Dreux, M., Garaigorta, U., Boyd, B., Decembre, E., Chung, J., Whitten-Bauer, C., Wieland, S., and Chisari, F.V. (2012). Short-range exosomal transfer of viral RNA from infected cells to plasmacytoid dendritic cells triggers innate immunity. Cell host & microbe *12*, 558-570.
Esashi, E., Bao, M., Wang, Y.H., Cao, W., and Liu, Y.J. (2012). PACSIN1 regulates the TLR7/9-mediated type I interferon response in plasmacytoid dendritic cells. European journal of immunology *42*, 573-579.
Guarda, G., Braun, M., Staehli, F., Tardivel, A., Mattmann, C., Forster, I., Farlik, M., Decker, T., Du Pasquier, R.A., Romero, P.*, et al.* (2011). Type I interferon inhibits interleukin-1 production and inflammasome activation. Immunity *34*, 213-223.
Hambleton, S., Salem, S., Bustamante, J., Bigley, V., Boisson-Dupuis, S., Azevedo, J., Fortin, A., Haniffa, M., Ceron-Gutierrez, L., Bacon, C.M.*, et al.* (2011). IRF8 mutations and human dendritic-cell immunodeficiency. N Engl J Med *365*, 127-138.
Hornell, T.M., Burster, T., Jahnsen, F.L., Pashine, A., Ochoa, M.T., Harding, J.J., Macaubas, C., Lee, A.W., Modlin, R.L., and Mellins, E.D. (2006). Human dendritic cell expression of HLA-DO is subset specific and regulated by maturation. Journal of immunology *176*, 3536-3547.
Hu, F., Yu, X., Wang, H., Zuo, D., Guo, C., Yi, H., Tirosh, B., Subjeck, J.R., Qiu, X., and Wang, X.Y. (2011). ER stress and its regulator X-box-binding protein-1 enhance polyIC-induced innate immune response in dendritic cells. European journal of immunology *41*, 1086-1097.
Hurst, J., Prinz, N., Lorenz, M., Bauer, S., Chapman, J., Lackner, K.J., and von Landenberg, P. (2009). TLR7 and TLR8 ligands and antiphospholipid antibodies show synergistic effects on the induction of IL-1beta and caspase-1 in monocytes and dendritic cells. Immunobiology *214*, 683-691.
Iwakoshi, N.N., Pypaert, M., and Glimcher, L.H. (2007). The transcription factor XBP-1 is essential for the development and survival of dendritic cells. The Journal of experimental medicine *204*, 2267-2275.
Janssens, S., Pulendran, B., and Lambrecht, B.N. (2014). Emerging functions of the unfolded protein response in immunity. Nature immunology *15*, 910-919.
Jongbloed, S.L., Kassianos, A.J., McDonald, K.J., Clark, G.J., Ju, X., Angel, C.E., Chen, C.J., Dunbar, P.R., Wadley, R.B., Jeet, V.*, et al.* (2010). Human CD141+ (BDCA-3)+ dendritic cells (DCs) represent a unique myeloid DC subset that cross-presents necrotic cell antigens. The Journal of experimental medicine *207*, 1247-1260.
Kivi, E., Elima, K., Aalto, K., Nymalm, Y., Auvinen, K., Koivunen, E., Otto, D.M., Crocker, P.R., Salminen, T.A., Salmi, M.*, et al.* (2009). Human Siglec-10 can bind to vascular adhesion protein-1 and serves as its substrate. Blood *114*, 5385-5392.
Li, N., Zhang, W., Wan, T., Zhang, J., Chen, T., Yu, Y., Wang, J., and Cao, X. (2001). Cloning and characterization of Siglec-10, a novel sialic acid binding member of the Ig superfamily, from human dendritic cells. J Biol Chem *276*, 28106-28112.
Lindstedt, M., Lundberg, K., and Borrebaeck, C.A. (2005). Gene family clustering identifies functionally associated subsets of human in vivo blood and tonsillar dendritic cells. Journal of immunology *175*, 4839-4846.
Luber, C.A., Cox, J., Lauterbach, H., Fancke, B., Selbach, M., Tschopp, J., Akira, S., Wiegand, M., Hochrein, H., O'Keeffe, M.*, et al.* (2010). Quantitative proteomics reveals subset-specific viral recognition in dendritic cells. Immunity *32*, 279-289.
Manh, T.P., Alexandre, Y., Baranek, T., Crozat, K., and Dalod, M. (2013). Plasmacytoid, conventional, and monocyte-derived dendritic cells undergo a

profound and convergent genetic reprogramming during their maturation. European journal of immunology *43*, 1706-1715.
Marafioti, T., Paterson, J.C., Ballabio, E., Reichard, K.K., Tedoldi, S., Hollowood, K., Dictor, M., Hansmann, M.L., Pileri, S.A., Dyer, M.J.*, et al.* (2008). Novel markers of normal and neoplastic human plasmacytoid dendritic cells. Blood *111*, 3778-3792.
Miller, J.C., Brown, B.D., Shay, T., Gautier, E.L., Jojic, V., Cohain, A., Pandey, G., Leboeuf, M., Elpek, K.G., Helft, J.*, et al.* (2012). Deciphering the transcriptional network of the dendritic cell lineage. Nature immunology *13*, 888-899.
Nepomuceno, R.R., and Tenner, A.J. (1998). C1qRP, the C1q receptor that enhances phagocytosis, is detected specifically in human cells of myeloid lineage, endothelial cells, and platelets. Journal of immunology *160*, 1929-1935.
Norsworthy, P.J., Fossati-Jimack, L., Cortes-Hernandez, J., Taylor, P.R., Bygrave, A.E., Thompson, R.D., Nourshargh, S., Walport, M.J., and Botto, M. (2004). Murine CD93 (C1qRp) contributes to the removal of apoptotic cells in vivo but is not required for C1q-mediated enhancement of phagocytosis. Journal of immunology *172*, 3406-3414.
Osorio, F., Tavernier, S.J., Hoffmann, E., Saeys, Y., Martens, L., Vetters, J., Delrue, I., De Rycke, R., Parthoens, E., Pouliot, P.*, et al.* (2014). The unfolded-protein-response sensor IRE-1alpha regulates the function of CD8alpha+ dendritic cells. Nature immunology *15*, 248-257.
Poulin, L.F., Salio, M., Griessinger, E., Anjos-Afonso, F., Craciun, L., Chen, J.L., Keller, A.M., Joffre, O., Zelenay, S., Nye, E.*, et al.* (2010). Characterization of human DNGR-1+ BDCA3+ leukocytes as putative equivalents of mouse CD8alpha+ dendritic cells. The Journal of experimental medicine *207*, 1261-1271.
Reynolds, G., and Haniffa, M. (2015). Human and Mouse Mononuclear Phagocyte Networks: A Tale of Two Species? Frontiers in immunology *6*, 330.
Robbins, S.H., Walzer, T., Dembele, D., Thibault, C., Defays, A., Bessou, G., Xu, H., Vivier, E., Sellars, M., Pierre, P.*, et al.* (2008). Novel insights into the relationships between dendritic cell subsets in human and mouse revealed by genome-wide expression profiling. Genome biology *9*, R17.
Rock, J., Schneider, E., Grun, J.R., Grutzkau, A., Kuppers, R., Schmitz, J., and Winkels, G. (2007). CD303 (BDCA-2) signals in plasmacytoid dendritic cells via a BCR-like signalosome involving Syk, Slp65 and PLCgamma2. European journal of immunology *37*, 3564-3575.
Salem, M., Mony, J.T., Lobner, M., Khorooshi, R., and Owens, T. (2011). Interferon regulatory factor-7 modulates experimental autoimmune encephalomyelitis in mice. Journal of neuroinflammation *8*, 181.
Schlatzer, D.M., Sugalski, J., Dazard, J.E., Chance, M.R., and Anthony, D.D. (2012). A quantitative proteomic approach for detecting protein profiles of activated human myeloid dendritic cells. Journal of immunological methods *375*, 39-45.
Segura, E., Valladeau-Guilemond, J., Donnadieu, M.H., Sastre-Garau, X., Soumelis, V., and Amigorena, S. (2012). Characterization of resident and migratory dendritic cells in human lymph nodes. The Journal of experimental medicine *209*, 653-660.
Stephenson, H.N., Mills, D.C., Jones, H., Milioris, E., Copland, A., Dorrell, N., Wren, B.W., Crocker, P.R., Escors, D., and Bajaj-Elliott, M. (2014). Pseudaminic acid on Campylobacter jejuni flagella modulates dendritic cell IL-10 expression via Siglec-10 receptor: a novel flagellin-host interaction. J Infect Dis *210*, 1487-1498.
Tailor, P., Tamura, T., Kong, H.J., Kubota, T., Kubota, M., Borghi, P., Gabriele, L., and Ozato, K. (2007). The feedback phase of type I interferon induction in dendritic cells requires interferon regulatory factor 8. Immunity *27*, 228-239.

Tailor, P., Tamura, T., Morse, H.C., 3rd, and Ozato, K. (2008). The BXH2 mutation in IRF8 differentially impairs dendritic cell subset development in the mouse. Blood *111*, 1942-1945.
Tel, J., Schreibelt, G., Sittig, S.P., Mathan, T.S., Buschow, S.I., Cruz, L.J., Lambeck, A.J., Figdor, C.G., and de Vries, I.J. (2013). Human plasmacytoid dendritic cells efficiently cross-present exogenous Ags to CD8+ T cells despite lower Ag uptake than myeloid dendritic cell subsets. Blood *121*, 459-467.
Theocharidis, A., van Dongen, S., Enright, A.J., and Freeman, T.C. (2009). Network visualization and analysis of gene expression data using BioLayout Express(3D). Nature protocols *4*, 1535-1550.
Vu Manh, T.P., Bertho, N., Hosmalin, A., Schwartz-Cornil, I., and Dalod, M. (2015). Investigating Evolutionary Conservation of Dendritic Cell Subset Identity and Functions. Frontiers in immunology *6*, 260.
Wu, X., Satpathy, A.T., Kc, W., Liu, P., Murphy, T.L., and Murphy, K.M. (2013). Bcl11a controls Flt3 expression in early hematopoietic progenitors and is required for pDC development in vivo. PloS one *8*, e64800.
Yu, C.F., Peng, W.M., Oldenburg, J., Hoch, J., Bieber, T., Limmer, A., Hartmann, G., Barchet, W., Eis-Hubinger, A.M., and Novak, N. (2010). Human plasmacytoid dendritic cells support Th17 cell effector function in response to TLR7 ligation. Journal of immunology *184*, 1159-1167.
Ziegler-Heitbrock, L., Ancuta, P., Crowe, S., Dalod, M., Grau, V., Hart, D.N., Leenen, P.J., Liu, Y.J., MacPherson, G., Randolph, G.J.*, et al.* (2010). Nomenclature of monocytes and dendritic cells in blood. Blood *116*, e74-80.

	Peptides D1	Peptides D2	Peptides D3
pDCs			
TLR9	**5**	**10**	**11**
IL3RA (CD123)	**2**	**3**	**7**
CLEC4C (BDCA2)	**0**	**2**	**4**
TLR7	**0**	**4**	**7**
NRP1 (BDCA4)	**1**	**0**	**1**
CD1c^{+}			
CD1C	**2**	**2**	**2**
BDCA3^{+}			
IDO1	**8**	**5**	**10**
TLR3	**3**	**0**	**0**
THBD^{a} (BDCA3)	**1**	**0**	**2**
CLEC9A^{a}	**0**	**1**	**0**
CD16^{+}			
FCGR3A (CD16)	**3**	**3**	**3**

Table 1. Subset identification markers uniquely identified.

Figure 1

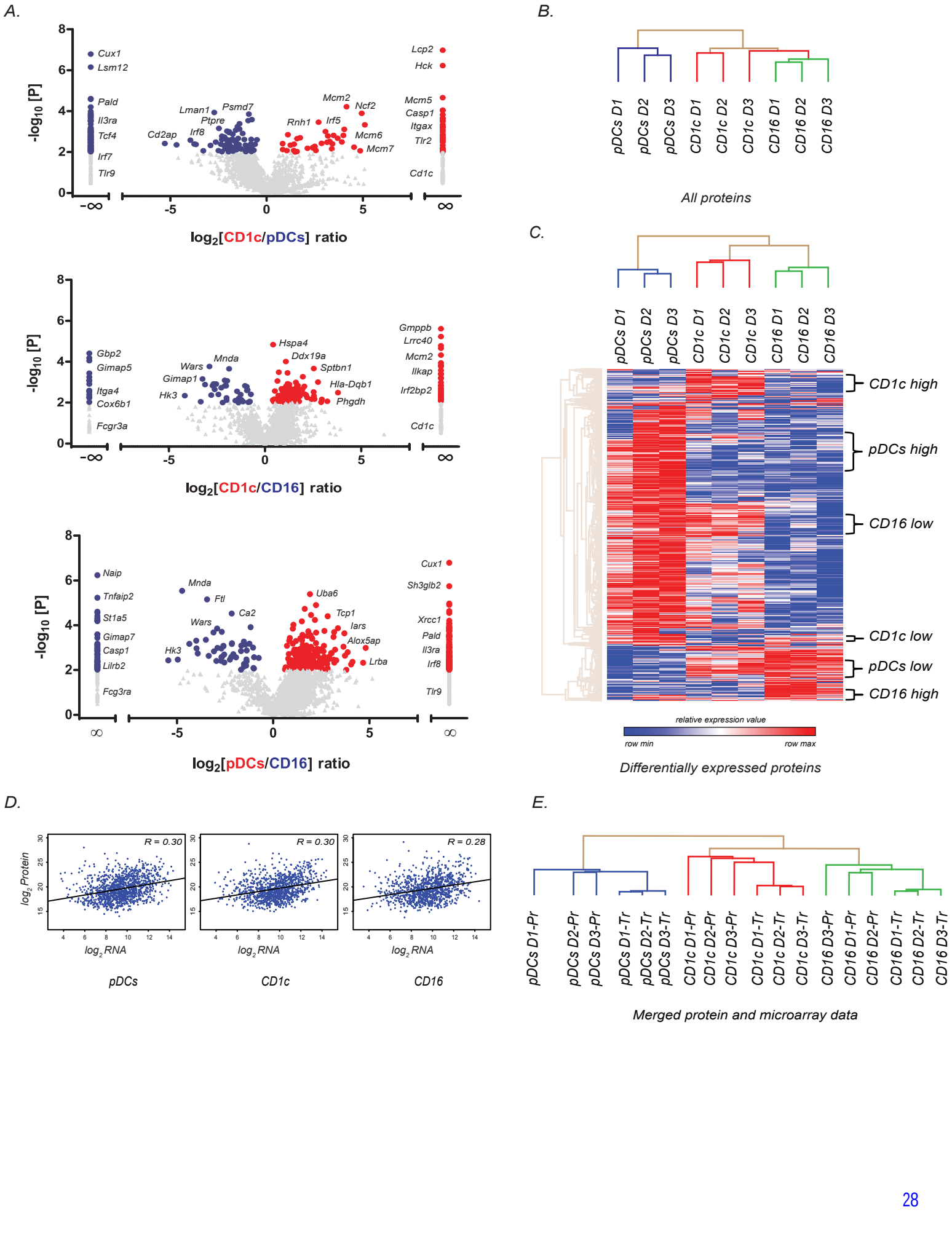
A.
-log10 [P]
Cux1
Lsm12
Pald
Il3ra
Tcf4
Irf7
Tlr9
Lman1
Psmd7
Ptpre
Cd2ap
Irf8
Mcm2
Ncf2
Rnh1
Irf5
Mcm6
Mcm7
Lcp2
Hck
Mcm5
Casp1
Itgax
Tlr2
Cd1c
log2[CD1c/pDCs] ratio
Gbp2
Gimap5
Itga4
Cox6b1
Fcgr3a
Wars
Mnda
Gimap1
Hk3
Hspa4
Ddx19a
Sptbn1
Hla-Dqb1
Phgdh
Gmppb
Lrrc40
Mcm2
Ilkap
Irf2bp2
Cd1c
log2[CD1c/CD16] ratio
Naip
Tnfaip2
St1a5
Gimap7
Casp1
Lilrb2
Fcg3ra
Mnda
Ftl
Wars
Ca2
Hk3
Uba6
Tcp1
Iars
Alox5ap
Lrba
Cux1
Sh3glb2
Xrcc1
Pald
Il3ra
Irf8
Tlr9
log2[pDCs/CD16] ratio
B.
pDCs D1
pDCs D2
pDCs D3
CD1c D1
CD1c D2
CD1c D3
CD16 D1
CD16 D2
CD16 D3
All proteins
C.
CD1c high
pDCs high
CD16 low
CD1c low
pDCs low
CD16 high
relative expression value
row min
row max
Differentially expressed proteins
D.
log2 Protein
log2 RNA
R = 0.30
R = 0.30
R = 0.28
pDCs
CD1c
CD16
E.
pDCs D1-Pr
pDCs D2-Pr
pDCs D3-Pr
pDCs D1-Tr
pDCs D2-Tr
pDCs D3-Tr
CD1c D1-Pr
CD1c D2-Pr
CD1c D3-Pr
CD1c D1-Tr
CD1c D2-Tr
CD1c D3-Tr
CD16 D3-Pr
CD16 D1-Pr
CD16 D2-Pr
CD16 D1-Tr
CD16 D2-Tr
CD16 D3-Tr
Merged protein and microarray data

Figure 2

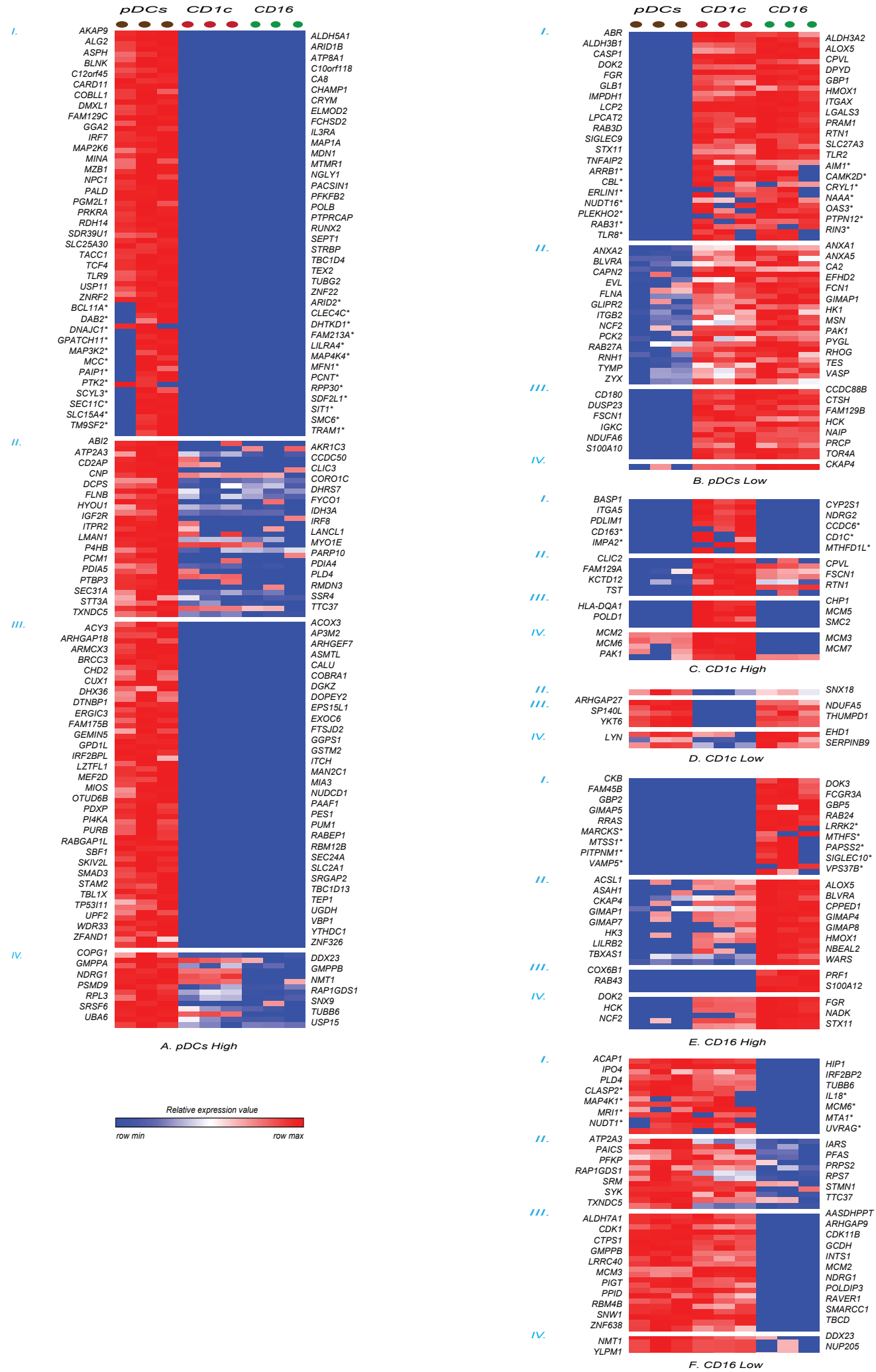
pDCs
CD1c
CD16
I.
AKAP9
ALG2
ASPH
BLNK
C12orf45
CARD11
COBLL1
DMXL1
FAM129C
GGA2
IRF7
MAP2K6
MINA
MZB1
NPC1
PALD
PGM2L1
PRKRA
RDH14
SDR39U1
SLC25A30
TACC1
TCF4
TLR9
USP11
ZNRF2
BCL11A*
DAB2*
DNAJC1*
GPATCH11*
MAP3K2*
MCC*
PAIP1*
PTK2*
SCYL3*
SEC11C*
SLC15A4*
TM9SF2*
ALDH5A1
ARID1B
ATP8A1
C10orf118
CA8
CHAMP1
CRYM
ELMOD2
FCHSD2
IL3RA
MAP1A
MDN1
MTMR1
NGLY1
PACSIN1
PFKFB2
POLB
PTPRCAP
RUNX2
SEPT1
STRBP
TBC1D4
TEX2
TUBG2
ZNF22
ARID2*
CLEC4C*
DHTKD1*
FAM213A*
LILRA4*
MAP4K4*
MFN1*
PCNT*
RPP30*
SDF2L1*
SIT1*
SMC6*
TRAM1*
II.
ABI2
ATP2A3
CD2AP
CNP
DCPS
FLNB
HYOU1
IGF2R
ITPR2
LMAN1
P4HB
PCM1
PDIA5
PTBP3
SEC31A
STT3A
TXNDC5
AKR1C3
CCDC50
CLIC3
CORO1C
DHRS7
FYCO1
IDH3A
IRF8
LANCL1
MYO1E
PARP10
PDIA4
PLD4
RMDN3
SSR4
TTC37
III.
ACY3
ARHGAP18
ARMCX3
BRCC3
CHD2
CUX1
DHX36
DTNBP1
ERGIC3
FAM175B
GEMIN5
GPD1L
IRF2BPL
LZTFL1
MEF2D
MIOS
OTUD6B
PDXP
PI4KA
PURB
RABGAP1L
SBF1
SKIV2L
SMAD3
STAM2
TBL1X
TP53I11
UPF2
WDR33
ZFAND1
ACOX3
AP3M2
ARHGEF7
ASMTL
CALU
COBRA1
DGKZ
DOPEY2
EPS15L1
EXOC6
FTSJD2
GGPS1
GSTM2
ITCH
MAN2C1
MIA3
NUDCD1
PAAF1
PES1
PUM1
RABEP1
RBM12B
SEC24A
SLC2A1
SRGAP2
TBC1D13
TEP1
UGDH
VBP1
YTHDC1
ZNF326
IV.
COPG1
GMPPA
NDRG1
PSMD9
RPL3
SRSF6
UBA6
DDX23
GMPPB
NMT1
RAP1GDS1
SNX9
TUBB6
USP15
A. pDCs High
Relative expression value
row min
row max
pDCs
CD1c
CD16
I.
ABR
ALDH3B1
CASP1
DOK2
FGR
GLB1
IMPDH1
LCP2
LPCAT2
RAB3D
SIGLEC9
STX11
TNFAIP2
ARRB1*
CBL*
ERLIN1*
NUDT16*
PLEKHO2*
RAB31*
TLR8*
II.
ANXA2
BLVRA
CAPN2
EVL
FLNA
GLIPR2
ITGB2
NCF2
PCK2
RAB27A
RNH1
TYMP
ZYX
III.
CD180
DUSP23
FSCN1
IGKC
NDUFA6
S100A10
IV.
ALDH3A2
ALOX5
CPVL
DPYD
GBP1
HMOX1
ITGAX
LGALS3
PRAM1
RTN1
SLC27A3
TLR2
AIM1*
CAMK2D*
CRYL1*
NAAA*
OAS3*
PTPN12*
RIN3*
ANXA1
ANXA5
CA2
EFHD2
FCN1
GIMAP1
HK1
MSN
PAK1
PYGL
RHOG
TES
VASP
CCDC88B
CTSH
FAM129B
HCK
NAIP
PRCP
TOR4A
CKAP4
B. pDCs Low
I.
BASP1
ITGA5
PDLIM1
CD163*
IMPA2*
II.
CLIC2
FAM129A
KCTD12
TST
III.
HLA-DQA1
POLD1
IV.
MCM2
MCM6
PAK1
CYP2S1
NDRG2
CCDC6*
CD1C*
MTHFD1L*
CPVL
FSCN1
RTN1
CHP1
MCM5
SMC2
MCM3
MCM7
C. CD1c High
II.
III.
IV.
ARHGAP27
SP140L
YKT6
LYN
SNX18
NDUFA5
THUMPD1
EHD1
SERPINB9
D. CD1c Low
I.
II.
III.
IV.
CKB
FAM45B
GBP2
GIMAP5
RRAS
MARCKS*
MTSS1*
PITPNM1*
VAMP5*
ACSL1
ASAH1
CKAP4
GIMAP1
GIMAP7
HK3
LILRB2
TBXAS1
COX6B1
RAB43
DOK2
HCK
NCF2
DOK3
FCGR3A
GBP5
RAB24
LRRK2*
MTHFS*
PAPSS2*
SIGLEC10*
VPS37B*
ALOX5
BLVRA
CPPED1
GIMAP4
GIMAP8
HMOX1
NBEAL2
WARS
PRF1
S100A12
FGR
NADK
STX11
E. CD16 High
I.
II.
III.
IV.
ACAP1
IPO4
PLD4
CLASP2*
MAP4K1*
MRI1*
NUDT1*
ATP2A3
PAICS
PFKP
RAP1GDS1
SRM
SYK
TXNDC5
ALDH7A1
CDK1
CTPS1
GMPPB
LRRC40
MCM3
PIGT
PPID
RBM4B
SNW1
ZNF638
NMT1
YLPM1
HIP1
IRF2BP2
TUBB6
IL18*
MCM6*
MTA1*
UVRAG*
IARS
PFAS
PRPS2
RPS7
STMN1
TTC37
AASDHPPT
ARHGAP9
CDK11B
GCDH
INTS1
MCM2
NDRG1
POLDIP3
RAVER1
SMARCC1
TBCD
DDX23
NUP205
F. CD16 Low

Figure 3

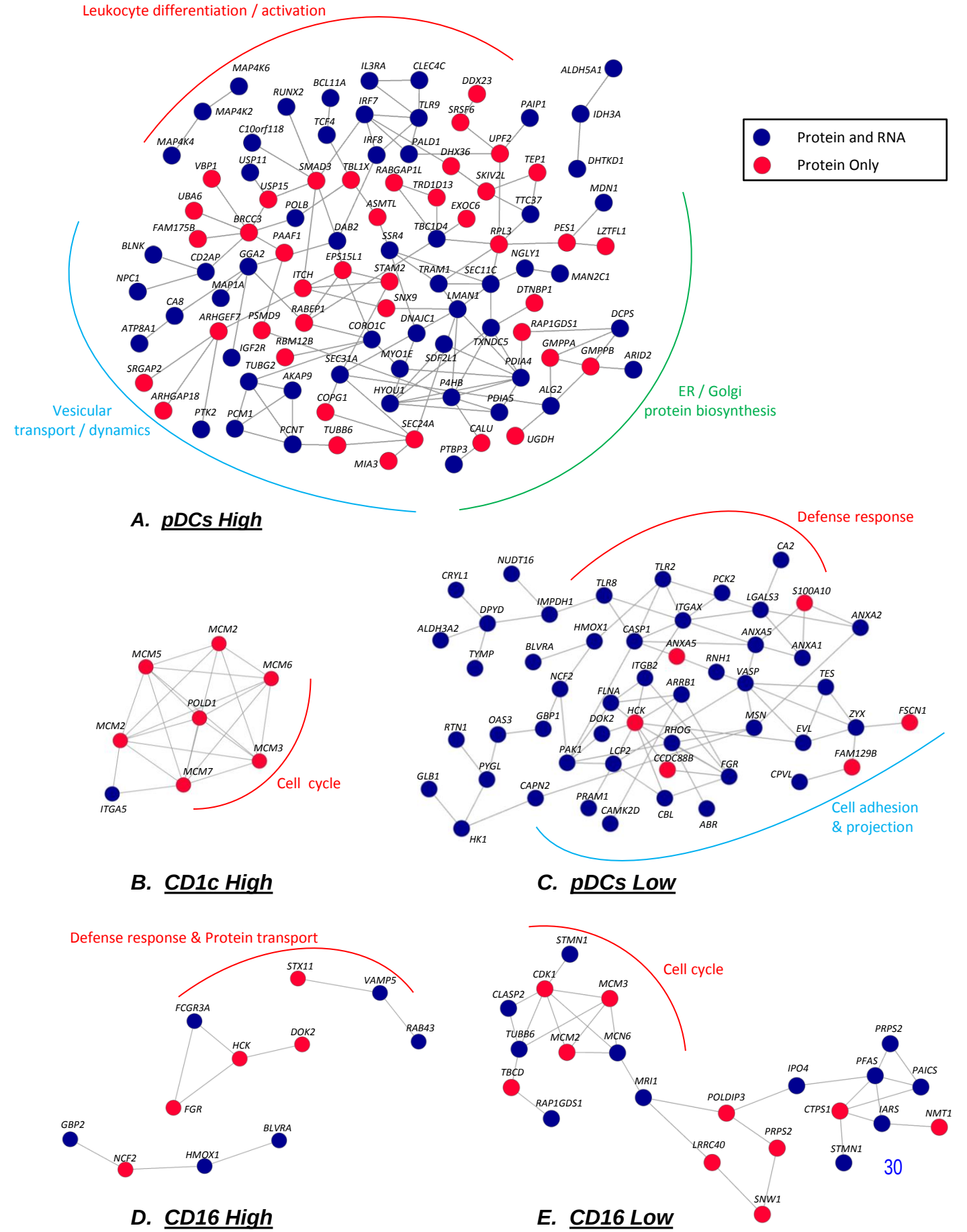
Leukocyte differentiation / activation
Vesicular transport / dynamics
ER / Golgi protein biosynthesis
Protein and RNA
Protein Only
A. pDCs High
Defense response
Cell cycle
Cell adhesion & projection
B. CD1c High
C. pDCs Low
Defense response & Protein transport
Cell cycle
D. CD16 High
E. CD16 Low

Figure 4

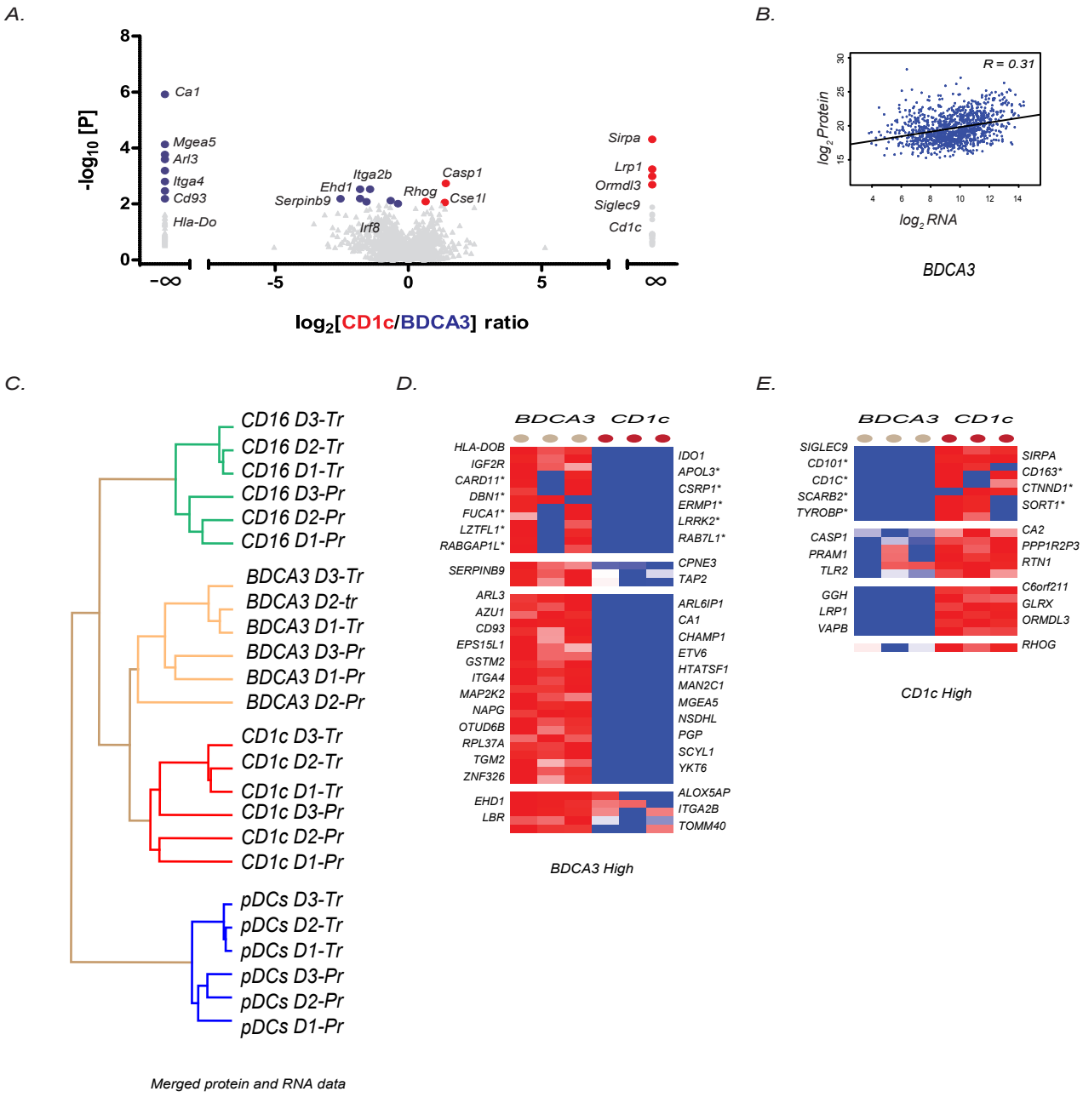
A.
B.
C.
D.
E.
-log10 [P]
Ca1
Mgea5
Arl3
Itga4
Cd93
Hla-Do
Itga2b
Ehd1
Serpinb9
Rhog
Casp1
Cse1l
Irf8
Sirpa
Lrp1
Ormdl3
Siglec9
Cd1c
log2[CD1c/BDCA3] ratio
R = 0.31
log2 Protein
log2 RNA
BDCA3
CD16 D3-Tr
CD16 D2-Tr
CD16 D1-Tr
CD16 D3-Pr
CD16 D2-Pr
CD16 D1-Pr
BDCA3 D3-Tr
BDCA3 D2-tr
BDCA3 D1-Tr
BDCA3 D3-Pr
BDCA3 D1-Pr
BDCA3 D2-Pr
CD1c D3-Tr
CD1c D2-Tr
CD1c D1-Tr
CD1c D3-Pr
CD1c D2-Pr
CD1c D1-Pr
pDCs D3-Tr
pDCs D2-Tr
pDCs D1-Tr
pDCs D3-Pr
pDCs D2-Pr
pDCs D1-Pr
Merged protein and RNA data
BDCA3 CD1c
HLA-DOB
IGF2R
CARD11*
DBN1*
FUCA1*
LZTFL1*
RABGAP1L*
IDO1
APOL3*
CSRP1*
ERMP1*
LRRK2*
RAB7L1*
SERPINB9
CPNE3
TAP2
ARL3
AZU1
CD93
EPS15L1
GSTM2
ITGA4
MAP2K2
NAPG
OTUD6B
RPL37A
TGM2
ZNF326
ARL6IP1
CA1
CHAMP1
ETV6
HTATSF1
MAN2C1
MGEA5
NSDHL
PGP
SCYL1
YKT6
EHD1
LBR
ALOX5AP
ITGA2B
TOMM40
BDCA3 High
SIGLEC9
CD101*
CD1C*
SCARB2*
TYROBP*
SIRPA
CD163*
CTNND1*
SORT1*
CASP1
PRAM1
TLR2
CA2
PPP1R2P3
RTN1
GGH
LRP1
VAPB
C6orf211
GLRX
ORMDL3
RHOG
CD1c High

Figure 5

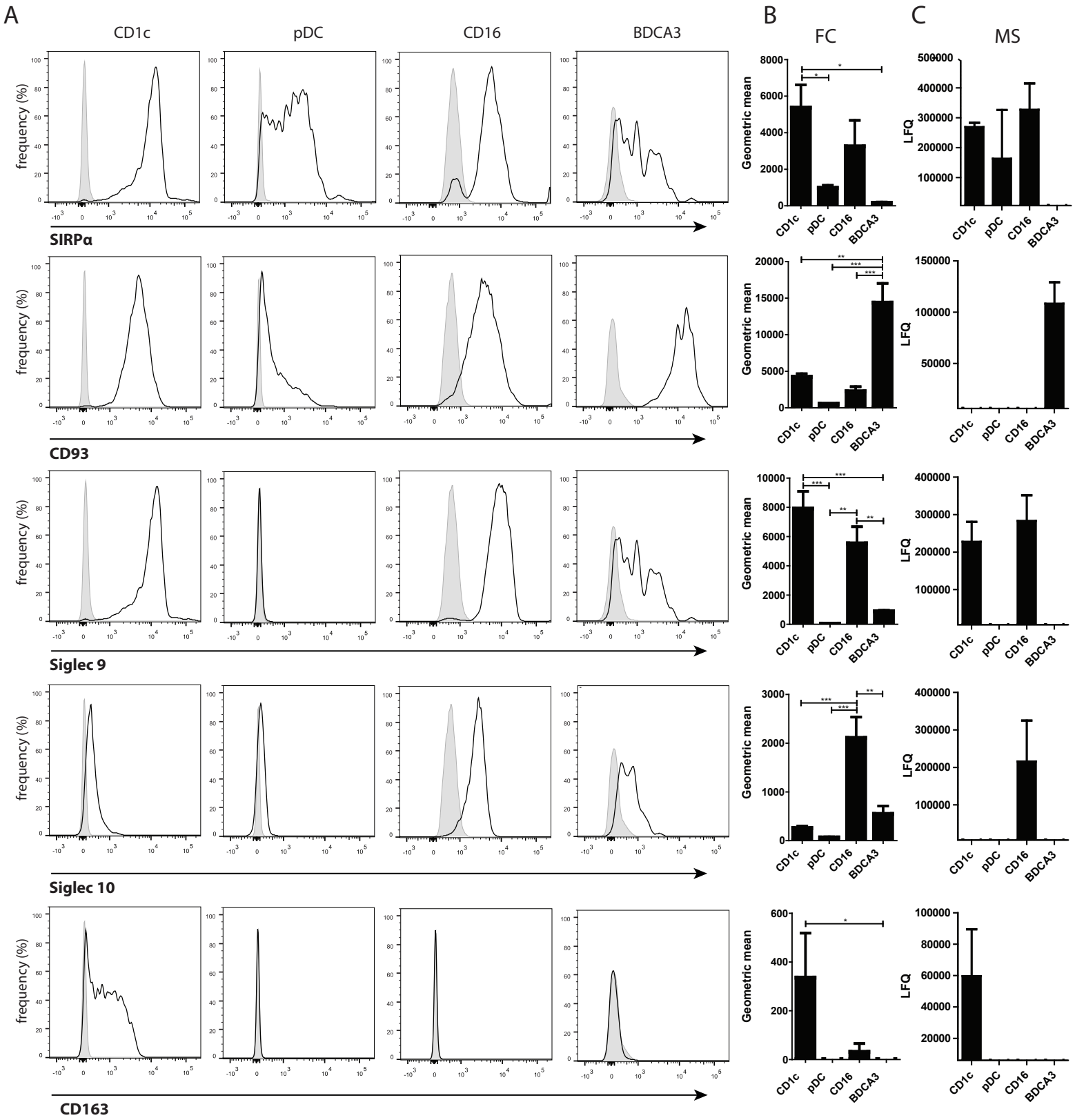
A
CD1c
pDC
CD16
BDCA3
B
FC
C
MS
frequency (%)
Geometric mean
LFQ
SIRPα
CD93
Siglec 9
Siglec 10
CD163
CD1c
pDC
CD16
BDCA3

Figure 6

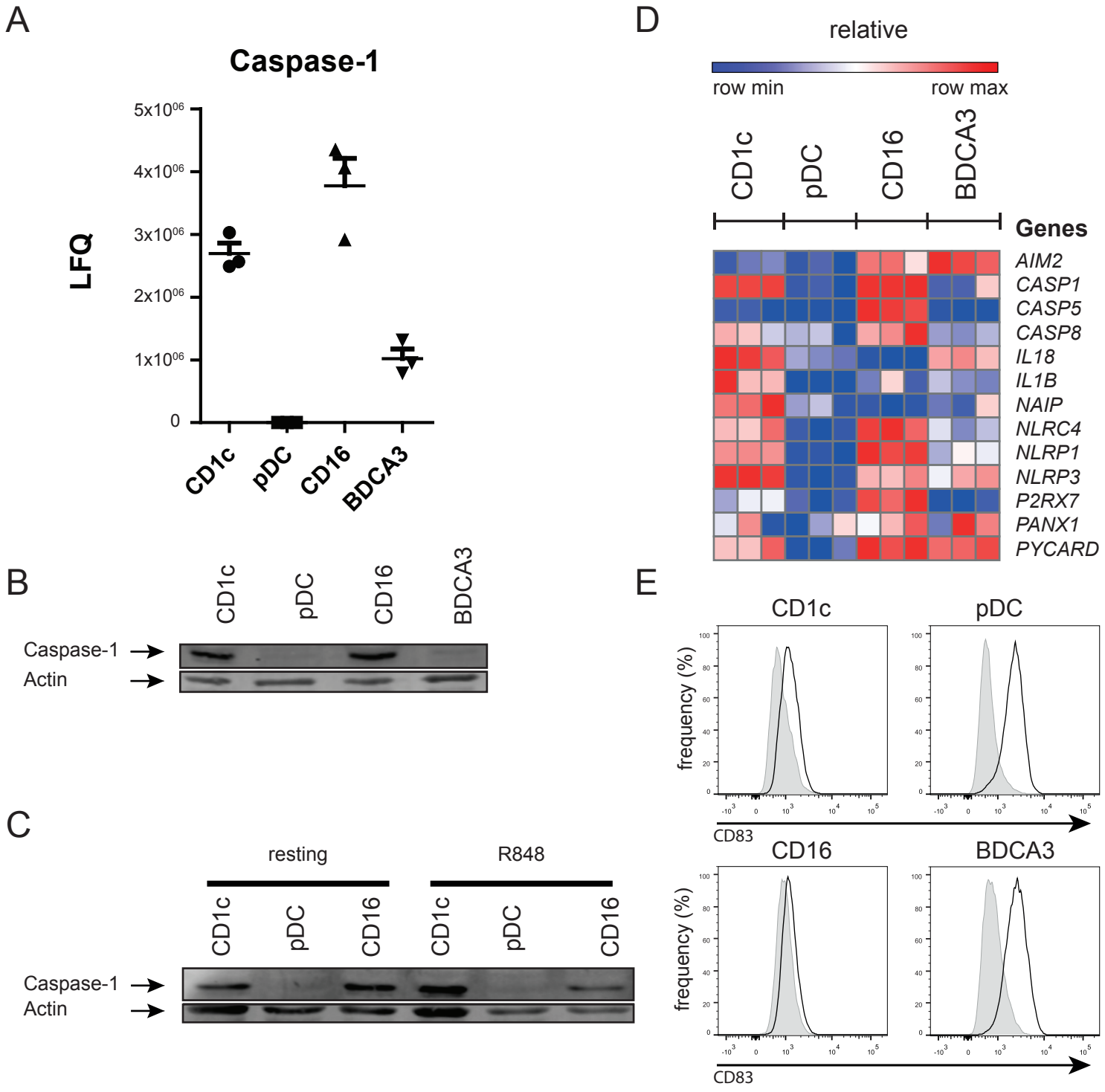
A
Caspase-1
LFQ
5x10^06
4x10^06
3x10^06
2x10^06
1x10^06
0
CD1c
pDC
CD16
BDCA3
B
CD1c
pDC
CD16
BDCA3
Caspase-1
Actin
C
resting
R848
CD1c
pDC
CD16
CD1c
pDC
CD16
Caspase-1
Actin
D
relative
row min
row max
CD1c
pDC
CD16
BDCA3
Genes
AIM2
CASP1
CASP5
CASP8
IL18
IL1B
NAIP
NLRC4
NLRP1
NLRP3
P2RX7
PANX1
PYCARD
E
CD1c
pDC
frequency (%)
CD83
CD16
BDCA3
frequency (%)
CD83
F
IL-1β (pg/ml)
TNFα (pg/ml)
G
IL-1β (pg/ml)
TNFα (pg/ml)
CD1c
CD1c R848/ATP
pDC
pDC R848/ATP
CD16
CD16 R848/ATP
BDCA3
BDCA3 R848/ATP

Supplemental data

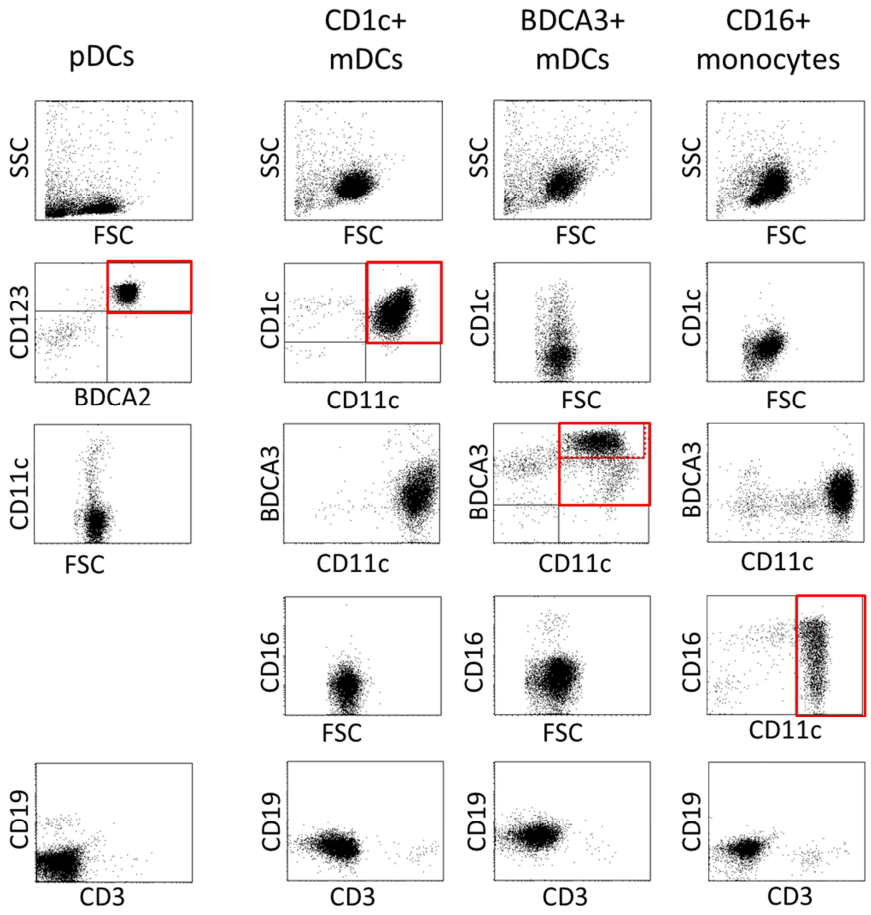

	pDC	CD1c+ mDC	BDCA3^{+}mDC (BDCA3^{hi} mDC)	CD16+ Monocytes
Donor 1	92%	95%	95% (45%)	98%
Donor 2	95%	98%	96% (83%)	96%
Donor 3	95%	78%	88% (49%)	82%

Figure S1 related to figures 1 and 3: Assessment of DC purity by flow cytometry: Flow cytometry results for magnetic bead purified subset samples. Displayed for one donor are the side-scatter (SSC) and forward-scatter (FSC; upper panel) and labelling for indicated subset identification markers (middle panels) and B (CD19) and T (CD3) cell markers (lower panels). For each subset the sorting gate used to quantify subset presence in the sample is marked by a red box. A summary of the percentage of each subset(of total cells) present in the samples from all donors used for MS analysis is given in the table. For BDCA3+ DCs values are provided both for total CD11c+BDCA3+ cells (red box) and CD11c+BDCA3^{hi} cells only (dotted red box). Please note that for the CD16+ monocyte sample, CD16 itself could not be used to reliably identify CD16+ cells after purification because of a decrease of CD16 label likely due to competition between the sorting antibody and the staining antibody. Therefore presence of CD16+ monocytes in this sample was based on CD11c only, which was justified by the concomitant absence of CD1c+ and BDCA3^{hi} cells.

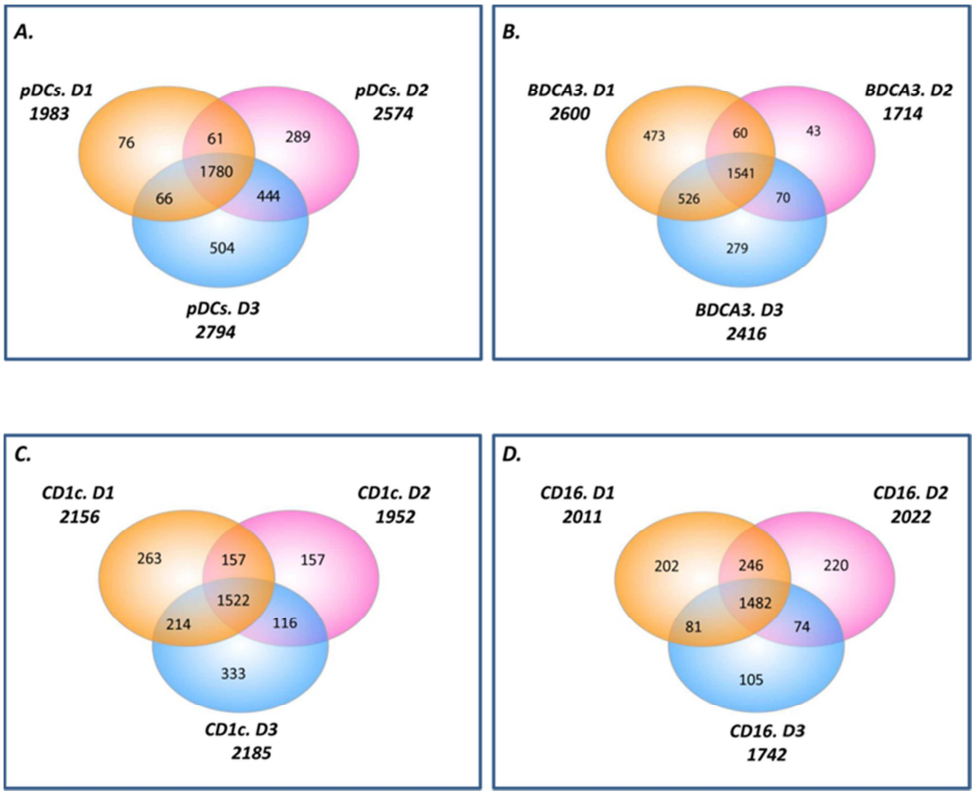

E.

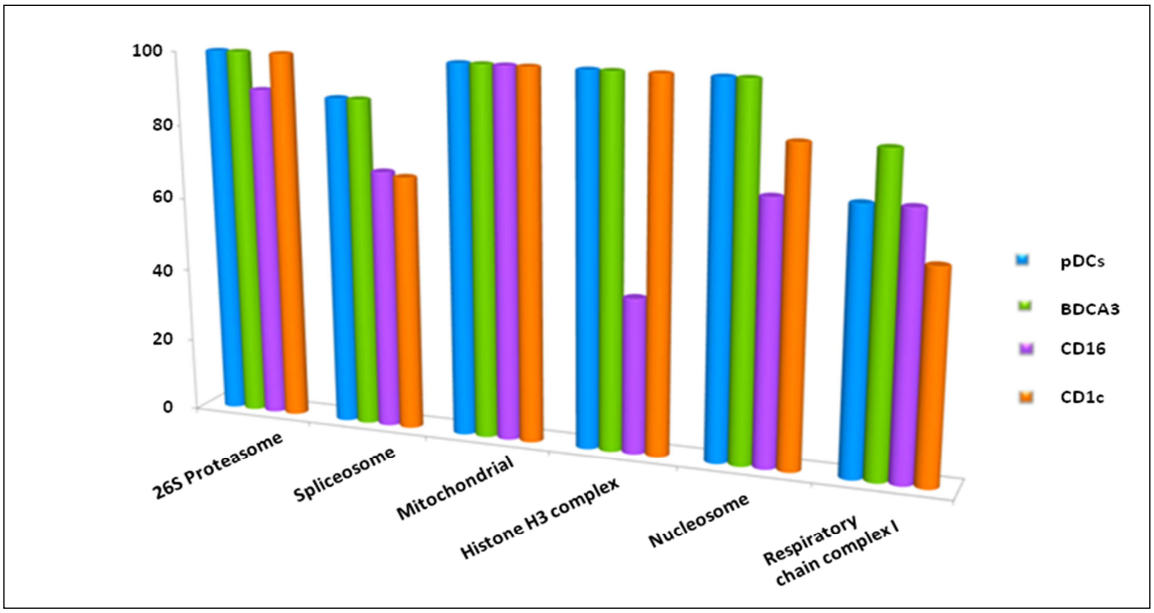

Figure S2 related to figures 1 and 3: Protein identification and coverage.
(A-D) Venn Diagrams representing the proteins identified in each donors for each subsets. (E)The percentage of complex components found back in each subset and donor for the indicated 6 essential protein complexes retrieved from the CORUM database. Coverage of these complexes provides a measure for the completeness of the measured proteome.

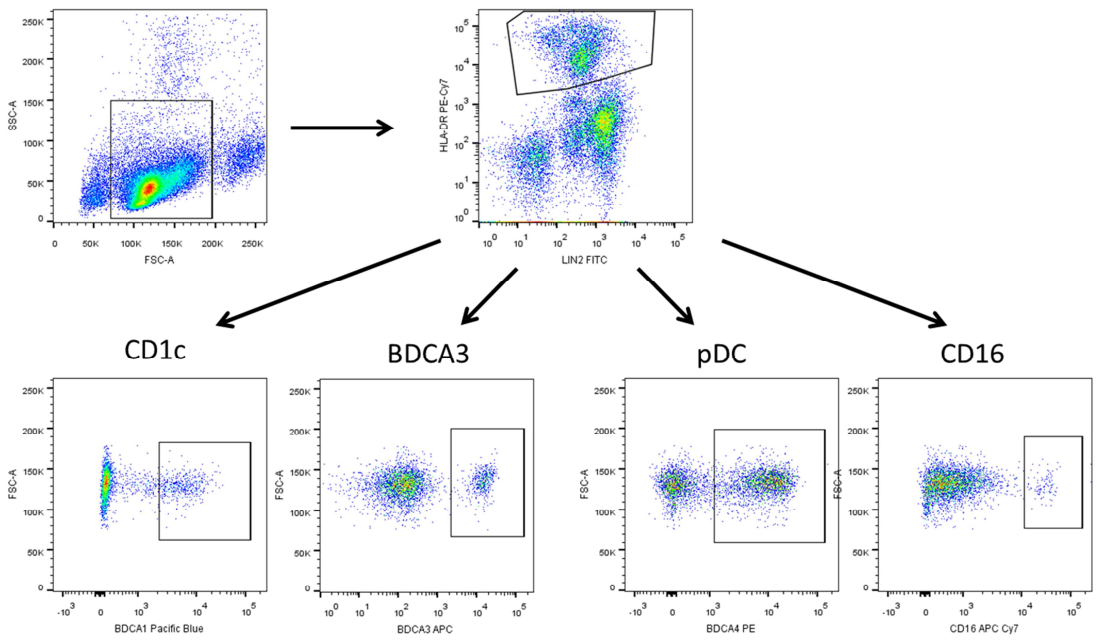

Figure S3 related to figure 6: Gating strategy for flow sorting of DC-subsets for Western blotting and functional analysis. A DC enriched fraction was obtained by magnetic bead depletion of non-DC PBMC constituents. This enriched fraction was subsequently sorted using a pool of lineage markers (CD3, CD14, CD16, CD19, CD20, and CD56; all excluded), HLA-DR (included) and the subset identification markers BDCA1, BDCA3, BDCA4 and CD16.

A

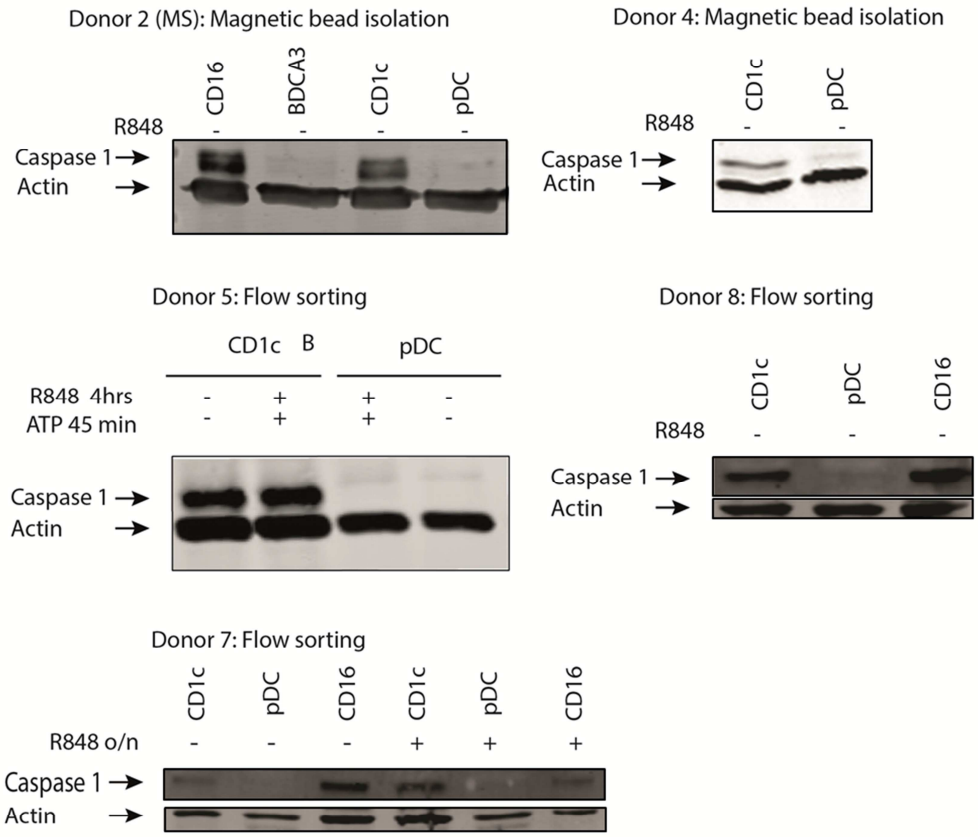

B

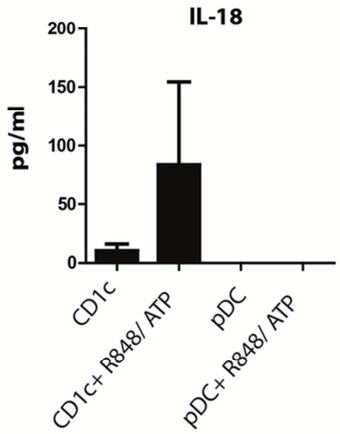

Figure S4 related to figure 6: Additional evidence for the absence of Caspase-1 and Caspase-1 dependent cytokine secretion in pDCs. (A) Additional Western blots for Caspase-1 and actin of magnetic bead isolated or flow cytometry sorted resting or R848 (ATP) stimulated DC-like subsets from one donor also used for MS analysis (donor 2) and 4 additional novel donors (4,5,7,8; Western blots of donors 6 and 9 are depicted in figure 6 of the main manuscript). (B) Presence of IL-18 in the supernatant of CD1c+ mDCs or pDCs measured by ELISA after stimulation for 4 hours with R848 followed by 45 minutes of ATP. Shown is the mean amount secreted by 3 donors +/- SEM.

Supplemental methods

Cells

For proteome analysis, DCs were isolated from aphaeresis products obtained from healthy volunteers after written informed consent and according to institutional guidelines. Peripheral Blood Mononuclear Cells (PBMCs) were purified from aphaeresis products via ficoll density gradient centrifugation (Lucron Bioproducts, Sint Martens-Latem, Belgium). To obtain peripheral blood leukocytes (PBLs), monocytes were depleted from PBMCs via adherence to plastic culture flasks. CD1c+ mDCs and CD16+ mDCs were isolated from PBMCs with a CD1c+ DC isolation kit and CD16+ monocyte isolation kit, respectively. BDCA3 myeloid DCs were isolated from PBLs by selection for BDCA3+ cells with a CD141 (BDCA3) isolation kit. Plasmacytoid DCs were purified from PBLs by positive selection using anti–BDCA-4–conjugated magnetic microbeads (all Miltenyi Biotec, Bergisch Gladback, Germany). DC purity was assessed by flow cytometry by staining for identification markers as indicated in Figure S1. Antibodies used for CD11c, CD1c, CD16+, BDCA3, BDCA2 and CD123 were all from Miltenyi Biotec and as described previously (Schreibelt et al., 2012; Tel et al., 2013). Contamination with T cells and B cells was assessed by double staining of CD19 and CD3 (BD Biosciences).

For Western blotting and ex vivo stimulation, DCs were isolated from PBMCs obtained from buffy coats of healthy donors after written informed consent and according to institutional guidelines. For these experiments, pDCs and CD1c mDCs were either isolated by flow sorting after an initial DC-enrichment using a DC-enrichment kit (Miltenyi Biotec) and subsequent DC-identificationusing Lin1-FITC (BD Biosciences; containing a pool of antibodies for CD3, CD14, CD16, CD19, CD20, and CD56; to be excluded) anti-HLA-DR-PE-Cy7 (positive selection) and anti-BDCA3-APC, anti-BDCA4-PE (B, pDCs) (all from Miltenyi), anti-CD16-APC-Cy7 (BD Biosciences) and anti-CD1c-PB (Biolegend). See figure S3A for the gating strategy. The four subsets were sorted using a FACS Aria II (BD Biosciences).For measuring the subset specific expression of 5 novel selected surface markers, PBMCs from healthy donors were stained for each of the surface marker using specific or isotype control antibodies conjugated to PE (below) and either a cocktail containing CD45-APC-Vio770, CD14-VioGreen, BDCA-3-APC, Clec9a-VioBrightFITC, CD20-PE-Vio770 (all from Miltenyi) CD1c-BV421 (Biolegend) to identify CD1c mDC (CD45+, CD20-, CD14-, BDCA1+) and BDCA3+ mDC (CD45+, CD20-, CD14-, BDCA3+, CLEC9A+), or a cocktail containing CD45-V450 (BD Biosciences), BDCA-2-APC, CD123-APC-Vio770 (both from Miltenyi), CD16-PE-Cy7, HLA-DR-BV510 and Lin2(CD56, CD3, CD14, CD20, CD19)-FITC (all from BD Biosciences) to identify pDCs (CD45+, Lin2-, HLA-DR+, BDCA2+, CD123+) and CD16+ monocytes (CD45+, Lin2-, HLA-DR+, CD16+). Selected novel surface markers were stained using PE-conjugated monoclonal antibodies against CD93 (Miltenyi Biotec), Siglec-9 (R&D systems), SIRPα (Biolegend), CD163 (BD Biosciences) and Siglec-10 (Biolegend).

Protein Extraction/Sample Preparation for MS

The purified and isolated DC subsets were resuspended in homogenisation buffer (20 mM Hepes (Roche) pH 7.5, 250 mM sucrose (Baker) and complete protease inhibitor cocktail (Roche)) and disrupted by three cycles of freezing and thawing. The cells were centrifuged at 10,000 g to separate soluble and insoluble fractions and separated by SDS-PAGE using precasted 4-20% TRIS/Bis ready Gels (Biorad). Both soluble and insoluble fractions were loaded onto gels for MS analysis. For each subset in total 8ug of protein was loaded corresponding to $5\text{-}10.10^5$ cells. After electrophoreses the protein gel was stained with Novex Colloidal Blue (Invitrogen) and each lane was cut in to ten fractions. Gel fractions were subsequently treated with dithiothreitol (DTT) and iodoacetamide and digested by trypsin. Digested samples were acidified to a final concentration of 0.5% HAc and purified by STAGE tips as described before (Rappsilber et al., 2003).

Liquid chromatography tandem mass spectrometry

All the samples were analyzed using liquid chromatography (Easy n-LC; Thermo Fisher scientific) coupled to a 7-T linear ion trap Fourier-Transform ion cyclotron resonance mass spectrometer model (LTQ FT Ultra, Thermo Fisher Scientific). Chromatography was performed with PicoTip columns (New Objective, Woburn, USA) of 15 cm 100 µm in size and was packed with 3 µm Reprosil C18 beads (Dr. Maisch). Tryptic peptides were separated using a 90 min gradient from 12% buffer B to 40 % buffer B (buffer B contains 80% acetonitrile in 0.5% acetic acid) with a flow-rate of 300 nL/min. The LTQ-FT instrument was operated in data-dependent mode. Full-scan MS spectra of intact peptides (m/z 350-1500) with an automated gain control accumulation target values of 1.000.0000 ions were acquired in the Fourier transform ion cyclotron resonance cell. The four most abundant ions were sequentially isolated and fragmented in the linear ion trap by applying collisional induced dissociation using an accumulation target value of 10.000, a capillary temperature of 100 ° C, and a normalized collision energy of 27%. A dynamic exclusion of ions previously sequenced was enabled. All unassigned charges states and singly charges ions were excluded from sequencing. A minimum of 200 counts was required for MS2

selection. Maximum injection times were set at 500 ms and 400 ms respectively for FT MS and IT MS/MS measurements.

Mass spectrometry data processing and protein identification
Proteins were identified and quantified from raw mass spectrometric files using MaxQuant software version 1.3.0.5 (Cox and Mann, 2008). Peak lists were generated to contain the six most intense peaks per 100 Dalton mass window. Database search was performed in Andromeda search engine (Cox et al., 2011) against Human Uniprot database (86,749 entries, June 2012) supplemented with sequences of contaminant proteins. We included cysteine carbamidomethylation as a fixed modification and oxidized-methionine and protein N-terminal acetylation as variable modifications. The minimum peptide length was six amino acids and up to two tryptic mis-cleavages were considered for identification. The time window of 2 minutes was allowed to match peptides across different LC-MS/MS run from each fraction on basis of mass and retention time. At least two peptides, of which one was unique, were required for the protein identification. Protein quantification was based on both unique and "razor" peptides. The protein abundance was determined by MaxLFQ that is based on comparison of individual peptide intensities over all samples as described by (Cox et al., 2014) and LFQ intensities values were normalized across biological replicates using median value. For ANOVA and hierchical clustering (below) missing values were filled by random values from the lower end of the expression value spectrum using Perseus software (version 1.4.2.23; Tyanova et al., 2016). Raw MS data are available at proteome central (accession number PXD004678) (http://proteomecentral.proteomexchange.org)

Statistical analysis of protein data
Since DC subsets derived from the third donor were of lower purity further use of these samples is only justified when sufficiently stringent criteria are used. Therefore, to extract reliable and informative data, observed protein expression differences were only used when present in at least two out of three donors or when confirmed by additional data from independent studies.
The list of differentially expressed proteins for hierarchical clustering and signature generation was obtained by merging subsets specifically expressed proteins (present in at least 2 out of 3 donors and absent in all other subsets in all donors) to proteins that were called significantly differentially expressed by 3-group one-way ANOVA (p-0.05) on the imputation supplemented protein data. On the ANOVA p-values a bonferoni-Holms correction for multiple testing was performed (Table S7). Furthermore, to prevent false positive results, proteins expressed below a measured LFQ value of 2^{17} were excluded from ANOVA because for these proteins the imputed LFQs to fill missing values may exceed that of the measured values. ANOVA was performed in the R programming environment.

Data processing of publically available transcriptome data
The raw microarray data (CEL files) were downloaded from ArrayExpress (accession: E-TABM-34) for human DC subsets (pDCs, BDCA3+ DCs, CD1c+ DCs, CD16+ cells). The raw data was normalized using the RMA normalization function of the affy package and mapped using hgu133plus2.db annotation package (Gautier et al., 2004). After data normalization, only the genes that had an expression level above background in at least 1 out of 4 populations with a differential expression between at least 2 cell types were considered. In cases where multiple probes were related to a gene, only the probe expressed highest across all samples was considered.

RNA sequencing
For RNA sequencing RNA was extracted from subsets lysed immediately after harvesting in Trizol reagent (Thermo fisher) and forcing the lysate trough a 25 gauge syringe for 10 times. RNA was subsequently isolated using and RNeasy kit and on-column DNase treatment (both from Qiagen). Thereafter for each sample 250 ng of total RNA was treated by Ribo-Zero rRNA Removal Kit (epicentre) to remove ribosomal RNAs (according to manufacturer instructions) and mRNA was purified using the (Zymo research). Subsequently purified RNA was fragmented using (5x) fragmentation buffer (200 mM Tris acetate pH 8.2, 500 mM potassium acetate and 150 mM magnesium acetate) and incubated at 95°C for 90 seconds. After a new round of purification, first strand cDNA was synthesized from fragmented RNA with SuperscriptIII (Invitrogen). First strand cDNA was purified by MinElute cleanup kit (Qiagen) and second strand cDNA was prepared in the presence of dUTP instead of dTTP and using random hexamers. Double stranded cDNA was purified by Qiagen mini elute columns and used for Illumina sample prepping and sequenced according to the manufacturer's instructions. The RNAseq reads were mapped to HG18 and used to calculate RPKM values (reads per kilobase of gene length per million reads) (Mortazavi et al., 2008).

Hierarchical clustering
The hierarchical clustering of samples and genes was performed based on 1-Pearson correlation in combination with average linkage clustering using GENE-E software (http://www.broadinstitute.org/cancer/software/GENE-E).Proteome and transcriptome data were mapped based on similarity of the gene symbol. Both datasets were

separately normalized and z-scored in the R programming environment (mean to 0 and variance to 1). From the merged dataset differentially expressed proteins we extracted (present in at least 2 out of 3 donors and absent in all other subsets in all donors plus proteins called significantly differentially expressed by 3-group one-way ANOVA (p-0.05). The thus obtained dataset was used for hierarchical clustering of samples.

Signature generation
For proteins highly or lowly expressed in each of the 3 subsets (pDCs, CD1c+ mDC, CD16+ monocytes), protein signatures were generated by combining protein and transcriptome data in 4 levels of evidence according to the criteria below (Table S7).

For the high expression signatures for each subset the criteria were:
Level I) specific proteins with RNA support. Protein: Is specifically expressed in the subset in 3 out of 3 donors but absent in all other subsets. RNA: MinMax >1.5 fold for linear values (for Log2 values, FC = $Log2(Min)_{cluster\text{-}subset(s)}$-$Log2(Max)_{other\ subsets}$> 0.58). Proteins specifically expressed only in 2 out of 3 donors were "rescued" and included in the signatures because of RNA support (MinMax >1.5 fold).
Level II) differentially expressed proteins with RNA support. Protein: 3-group one-way ANOVA proteomics with multiple testing correction (BH) <0.05 and expression in the subset(s) in at least 2 out of 3 donors. Post-hoc t-test comparisons proteomics for the high expressing subset(s) against other subset p<0.05 and a fold change of >2. RNA: MinMax >1.5 fold for linear values. ANOVA significant proteins (p<0.05) lost by multiple testing correction but meeting all other criteria and supported by RNA expression (MinMax >1.5 fold) were included in Table S7 as low confidence DEPs.
Level III) Specific protein expression without RNA support. Protein: As level I. RNA: Criteria Level I are not met or no data available. Proteins specifically expressed in only 2 out of 3 donors were also included Table S7 as low confidence DEPs
Level IV) Differential protein expression without RNA support. Protein as in level II; RNA: Conditions level II are not met or no data available.

For the proteins lowly expressed in subset the criteria were as above with the following modifications:
Level I) Protein: Absent in the cluster-subset but present in all other subsets; RNA: Minimum expression in other subsets over maximum in the subset > 1.5 fold. Proteins absent in the cluster-subset in 3/3 donors but present in only 2/ 3 donors in (any of) the other subsets are
included in Table S7 as low confidence DEPs.
Level II) Protein: Presence in the other subset in at least 2 out of 3 donors.
Level III) Protein as for level I. Proteins absent in the cluster-subset in 3/3 donors but present in only 2/ 3 donors in (any of) the other subsets were also included in Table S7 as low confidence DEPs.
Level IV) Protein as for level II. RNA: Did not meet criteria level II or no data available.

Finally, proteins identified in at least two donors in one subset but not identified as differentially expressed according to the signature criteria above, yet found differntially expressed based on RNA expression data are given in supplementary table S8.

Extracting DEPs between BDCA3+ mDCs and CD1c+ mDCs:
To extract DEPs we aplied roughly the same structure as for signature generation but now based on t-tests and with the follwing specific rules:
Level I: present in > 2/3 donors in one of the 2 subsets, no presence in the other subset (3/3), also significant at RNA level by Min Max (> 1.5 fold)
Level II: t-test significant (p-value <0.05, FC >2), also significant at RNA by Min max (> 1.5 fold)
Level III: present in > 3/3 donors in one of the 2 subsets, no presence in the other subset (3/3), no RNA data or significance. Proteins only specifically present in 2/3 donors are only present in Table S7 as low confidence DEPs
Level IV: t-test significant (p-value < 0.01, FC>2); no presence in the other subset (3/3), no RNA data or significance. Proteins with a t-test p-value between 0.01 and 0.05 are only present in Table S7 as low confidence DEPs

Protein-protein Interaction, GO and pathway analysis
Signatures depicted in figure 2 were used as input for protein-protein interaction (PPI) analysis using the STRING PPI web tool (http://string-db.org/; version 10). A confidence score of 0.4 was used as a cut-off for protein-protein interaction allowing all sources of evidence. Obtained confidence scores for each interaction can be found in table S9. The generated interaction networks were uploaded in Biolayout express 3D (version 3.3) for graphical representation (Theocharidis et al., 2009). Signatures were mapped onto functional categories

using the functional annotation clustering algorithm in the DAVID web tool (https://david.ncifcrf.gov/) using standard settings. Full functional annotation output can be found in Table S9.

Western blotting
Reduced cells lysates were loaded on a 10% SDS-gel and transferred to a PVDF membrane. Caspase-1 was stained with the caspase-1-p10 (C-20): sc-515 antibody (Santa Cruz Biotechnology) and Actin with anti-Actin (20-33) antibody (Sigma). Blots were analyzed on the Odyssey imaging system.

ELISA
Cytokine production of IL-1β (R&D Systems) and TNF (eBioscience) was measured by ELISA. IL-18 production was analyzed by using Luminex. To monitor activation, cells were stained for 30 minutes with anti-CD83-FITC (BD Biosciences) and analyzed by flow cytometry.

Supplemental references

Cox, J., Hein, M.Y., Luber, C.A., Paron, I., Nagaraj, N., and Mann, M. (2014). Accurate proteome-wide label-free quantification by delayed normalization and maximal peptide ratio extraction, termed MaxLFQ. Mol Cell Proteomics *13*, 2513-2526.
Cox, J., and Mann, M. (2008). MaxQuant enables high peptide identification rates, individualized p.p.b.-range mass accuracies and proteome-wide protein quantification. Nat Biotechnol *26*, 1367-1372.
Cox, J., Neuhauser, N., Michalski, A., Scheltema, R.A., Olsen, J.V., and Mann, M. (2011). Andromeda: a peptide search engine integrated into the MaxQuant environment. Journal of proteome research *10*, 1794-1805.
Tyanova, S., Temu, T., Sinitcyn, P., Carlson, A., Hein, M.Y., Geiger, T., Mann, M., and Cox, J. (2016). The Perseus computational platform for comprehensive analysis of (prote)omics data. Nat Methods.
Gautier, L., Cope, L., Bolstad, B.M., and Irizarry, R.A. (2004). affy--analysis of Affymetrix GeneChip data at the probe level. Bioinformatics *20*, 307-315.
Mortazavi, A., Williams, B.A., McCue, K., Schaeffer, L., and Wold, B. (2008). Mapping and quantifying mammalian transcriptomes by RNA-Seq. Nat Methods *5*, 621-628.
Rappsilber, J., Ishihama, Y., and Mann, M. (2003). Stop and go extraction tips for matrix-assisted laser desorption/ionization, nanoelectrospray, and LC/MS sample pretreatment in proteomics. Anal Chem *75*, 663-670.
Schreibelt, G., Klinkenberg, L.J., Cruz, L.J., Tacken, P.J., Tel, J., Kreutz, M., Adema, G.J., Brown, G.D., Figdor, C.G., and de Vries, I.J. (2012). The C-type lectin receptor CLEC9A mediates antigen uptake and (cross-)presentation by human blood BDCA3+ myeloid dendritic cells. Blood *119*, 2284-2292.
Tel, J., Schreibelt, G., Sittig, S.P., Mathan, T.S., Buschow, S.I., Cruz, L.J., Lambeck, A.J., Figdor, C.G., and de Vries, I.J. (2013). Human plasmacytoid dendritic cells efficiently cross-present exogenous Ags to CD8+ T cells despite lower Ag uptake than myeloid dendritic cell subsets. Blood *121*, 459-467.
Theocharidis, A., van Dongen, S., Enright, A.J., and Freeman, T.C. (2009). Network visualization and analysis of gene expression data using BioLayout Express(3D). Nature protocols *4*, 1535-1550.

Overview of supplemental Tables:

Table S1: Correlation between biological and technical replicates_related to figures 1 and 4
Tab1: Technical replicates
Tab2: biological replicates
Table S2: Identified proteins_related to figures 1 and 4: Protein table of all proteins identified in all 4 subsets and all 4 donors (at least 2 in one subsets, no LFQ restrictions)

Table S3: Identified peptides_related to figures 1 and 4: Peptide table of all peptides identified in all 4 subsets in all 4 donors
Table S4: Pairwise comparison of subsets_related to figures 1 and 4: t-test of all combinations of all 4 subsets
Table S5: RNA sequencing data donor 2_related to figures 1 and 4
Table S6: Merged RNA and protein data_related to figures 1 and 4
Tab1: merged table RNA and protein data (MA and RNA seq)
Tab2: correlation of RNA (MA and RNA seq)
Table S7: Signatures_related to figures 2 and 4: Signatures for all 6 groups in the 3 subset comparison and for BDCA3 compared to CD1c+ mDC
Tab1: pDC vs CD1c & CD16 up
Tab2: pDC vs CD1c & CD16 down
Tab3: CD1c vs pDC& CD16 up
Tab4: CD1c vs pDC% CD16 down
Tab5: CD16vs pDC&CD1c up
Tab6: CD16 vs pDC&CD1c down
Tab7: BDCA3 vs CD1c up
Tab8: CD1c vs BDCA3 up
Table S8: Table S8_DEGs not confirmed by proteomics_related to figure 2 and 4
Tab1: pDC vs CD1c & CD16 up
Tab2: pDC vs CD1c & CD16 down
Tab3: CD1c vs pDC& CD16 up
Tab4: CD1c vs pDC% CD16 down
Tab5: CD16vs pDC&CD1c up
Tab6: CD16 vs pDC&CD1c down
Tab7: BDCA3 vs CD1c up
Tab8: CD1c vs BDCA3 up
Table S9: PPI and FA analysis_ related to figure 3
Tab1: pDC vs CD1c & CD16 up
Tab2: pDC vs CD1c & CD16 down
Tab3: CD1c vs pDC& CD16 up
Tab4: CD1c vs pDC% CD16 down
Tab5: CD16vs pDC&CD1c up
Tab6: CD16 vs pDC&CD1c down
Tab7: BDCA3 vs CD1c up
Tab8: CD1c vs BDCA3 up